University of Alberta

The Role of Sulfur during the Cracking of n-Hexadecane and Cold Lake Bitumen with alpha-Fe_2O_3 and Steam

by

Blake Jeremy Olson

A thesis submitted to the Faculty of Graduate Studies and Research
in partial fulfillment of the requirements for the degree of

Master of Science
in
Chemical Engineering

Department of Chemical and Materials Engineering

©Blake Jeremy Olson
Spring 2013
Edmonton, Alberta

Permission is hereby granted to the University of Alberta Libraries to reproduce single copies of this thesis and to lend or sell such copies for private, scholarly or scientific research purposes only. Where the thesis is converted to, or otherwise made available in digital form, the University of Alberta will advise potential users of the thesis of these terms.

The author reserves all other publication and other rights in association with the copyright in the thesis and, except as herein before provided, neither the thesis nor any substantial portion thereof may be printed or otherwise reproduced in any material form whatsoever without the author's prior written permission.

Abstract

Coke produced during bitumen upgrading has a high heteroatom content and low economic value. To improve feed efficiency, cracking of hexadecane and bitumen with α-Fe_2O_3 and water has been studied to decrease coke yield, while increasing sulfur content. Compared to thermal cracking, catalytic cracking of hexadecane with α-Fe_2O_3 increased the conversion by 11.8% overall. By adding steam, however, the conversion decreased by 5.9%, due to competitive adsorption. The reaction of H_2S with α-Fe_2O_3 was also inhibited by steam that competed for active sites and even oxidized the produced iron sulfides. Conversely, during bitumen cracking, α-Fe_2O_3 did not affect the coke yield due to fouling of the surface, but did increase the sulfur content of the solid product. On the other hand, the addition of water not only decreased the coke yield by ~3%, but also inhibited the reaction of H_2S, indicating that competitive adsorption was still occurring after fouling.

Acknowledgments

I would like to acknowledge and thank all those who have supported and helped me from the day I began this project till the day I wrote my final thought.

To my parents and beautiful wife Lauren, I would like to thank you most of all for your support, patience and love during all of my ups and downs. Without you this stressful and strenuous time period would have been nearly unbearable.

Thank you to Shaofeng, Gonzalo and Rosa for your assistance in the lab. Thanks to the CME machine shop for helping with the construction of all my materials, I would never have finished without you.

Thank you to my supervisors Dr. William McCaffrey and Dr. Arno De Klerk for putting your faith in me. Thank you for you assistance and for pushing me to achieve what I did not think I could achieve. I am a better person and engineer because of it.

Finally thank you to all of my friends for making this an enjoyable experience and for putting up with my quirks. Thank you to Brenden, Jessie and Paul for always being up for a morning coffee and putting up with my endless rants.

Table of Contents

List of Tables

List of Figures

List of Abbreviations

---

c	coke
CHNS	Carbon, Hydrogen, Nitrogen and Sulfur Elemental Analysis
Fe	α-Fe_2O_3
g	Gas
GC	Gas chromatography
l	Liquid
MS	Mass Spectrometry
NC	No Catalyst
NW	No Water
PVDF	Polyvinylidene fluoride
rpm	Rotations per minute
RO	Reverse Osmosis
s	Sulfur
SS	Stainless Steel
W	Water
XPS	X-Ray Photoelectron Spectroscopy
XRD	X-Ray Diffraction

Chapter 1: Introduction and Objectives

The Alberta Oil Sands contain more than 176 billion barrels of economically recoverable bitumen.[1] Delayed coking is the technology typically used as the primary upgrading step in the production of a high value liquid product.[2] However, this technology also produces gaseous hydrocarbons as well as a carbon rich solid known as coke.[2] Unfortunately, this solid has a reduced value due to its high heteroatom (Sulfur, Nitrogen and Oxygen) content and is subsequently stockpiled, resulting in a decreased feed efficiency.[2] It would therefore be useful to reduce the yield of coke, while maintaining a higher quality liquid product. Furthermore, given that the gaseous and liquid hydrocarbons produced will also have a significant heteroatom content, which must be removed, it would be ideal if the heteroatom pathway could be shifted to further increase within the coke.

Previous work has shown that water[3, 4] and solids[5-7] added during the coking process can reduce coke formation. While the use of water with α-Fe_2O_3,[8] ZrO_2-Al_2O_3-FeO_x[9-11] or Iron (II) Sulfate Heptahydrate[4] can reduce the coke yield further. It is also known that iron oxides such as α-Fe_2O_3 are capable of reacting with H_2S to produce Iron Sulfides.[12,13] It is therefore hypothesized that, cracking bitumen in the presence of α-Fe_2O_3 and water, may result in a coke with a reduced yield and increased sulfur content. Therefore, the objective of this study will be to investigate the decomposition of the model compound n-hexadecane and Cold Lake bitumen with α-Fe_2O_3 and water while examining the role sulfur plays in the decomposition.

Chapter 2: Literature Review

2.1 What is Bitumen?

Bitumen is a naturally occurring hydrocarbon resource associated with the Alberta oil sands. It is estimated that there are currently 176 billion barrels of economically recoverable bitumen, or approximately 10% of the total barrels in place,[1] with some estimates being placed as high as 2.5 trillion barrels.[14] With the global demand for energy increasing and feeds becoming heavier,[15] bitumen has become a valuable and viable resource. However, to make use of bitumen, cleaner and more efficient processes are required.

Bitumen is defined as:[16]

- Specific gravity>1
- API°<10
- Viscosity>10^4 mPa

These properties, as well as its chemical composition, make bitumen a unique and difficult feedstock to work with. Unlike many crude oils, bitumen contains no alkanes due to bacterial degradation[17] and the only saturated aliphatic chains are branched and attached to larger aromatic molecules, such as asphaltenes.[16] The lack of saturated hydrocarbons implies that bitumen has a low hydrogen to carbon ratio (Table 2-1). Table 2-1 presents the typical elemental composition of bitumen.[16] Across all types of bitumen, the amount of carbon and hydrogen is nearly constant, whereas the relative amount of the heteroatoms (Nitrogen, Oxygen, Sulfur, etc.) can vary substantially.

Table 2-1 Typical elemental composition of bitumen*

Element	Wt%
Carbon	83.1±0.5
Hydrogen	10.3±0.3
Nitrogen	0.4±0.1
Oxygen	1.1±0.3
Sulfur	4.5±0.5
H/C (Atomic ratio)	1.54-1.65

*Adapted from Strausz and Lown[16]

2.2 Upgrading of Bitumen

In order to create a high value product the H/C ratio must be increased while the heteroatom content must be decreased. For example, gasoline has an H/C of 1.9-1.95, implying that a significant amount of upgrading must be completed, to obtain a high quality value added product.[16] To increase the H/C ratio, the primary upgrading of bitumen and other heavy oils is completed using either hydrogen addition or carbon rejection technologies. Sawarkar *et al*. describes hydrogen addition as the reaction between the feed and an external hydrogen source, while carbon rejection reallocates the hydrogen to produce hydrogen rich and hydrogen poor fractions.[18] Although hydrogen addition technologies are capable of producing a high quality product, the large investment, high hydrogen requirements and overall complexity make it a less popular choice compared to carbon rejection technology.[18] Carbon rejection technologies, such as delayed coking, are far more common due to lower overall cost, ease of operations and their ability to handle almost any feed.[18] The production of a liquid product of higher quality than the feed comes at the cost of rejecting a significant amount of the feed as coke, an insoluble solid with a low H/C.[18] Oil sands coke, has a high heteroatom content and is thus typically stockpiled, lowering the feed efficiency.[2] It would therefore be ideal if the coke yield and H/C could be decreased to make the process more efficient.

2.3 Coking of Bitumen

Wiehe suggests that coke is formed through a series of reactions beginning with the cracking of asphaltenes and non-volatile heptane solubles to produce volatiles, heptane solubles and asphaltene cores.[19] Eventually the concentration of asphaltene cores within the liquid phase will exceed the solubility limit and form a second phase.[19] Within the new phase the concentration of abstractable hydrogen is minimal, causing radical addition reactions to become dominant and leading to the formation of coke.[19] Brooks and Taylor observed that when heated at temperatures over 400°C, an isotropic pitch begins to form small anisotropic spheres which grow in size upon further heating.[20] They attributed this to the separation of a second liquid phase, similar to that proposed by Wiehe.[20] Pyrolysis of a feed with increasing concentrations of asphaltenes showed that as the concentrations of asphaltenes increase, so too does the size of coke, consistent with increased coalescence.[21] Based on this theory, numerous studies have looked at the use of additives to inhibit coke formation as well as the coke yield.

Recognizing that Athabasca bitumen contains approximately 1.8 wt% of mineral solids, Tanabe and Gray hypothesized that the solids could act as a nucleation site for coke.[6] They found that the addition of solids resulted in an increased induction time for coke formation and supports the results of Bi and Gray, where coke yield was significantly reduced under short reaction times in the presence of fine solid.[22] Bi and Gray attributed this to the solids accumulating at the oil-coke interface preventing the coalescence of coke particles.[22] Similarly, during the cracking of asphaltenes with solids, less coalescence was observed when compared to cracking in the absence of fine solids.[21] The decreased particle size was attributed to the solids providing nucleation sites for the coke precursors, which would provide better dispersion and increased interaction with hydrogen donating molecules.[21] Hydrogen donation by molecules such as tetralin has been observed to reduce coke yield compared to solvents such as 1-Methylnaphthalene and maltene.[23] When examining the role of solids, Rahimi *et al*. observed that mesophase growth is suppressed in the presence of kaolinite more so than with montmorillonite and illite, highlighting the importance of the type of solid.[7] Similar results have been noticed when comparing $FeCl_3$-graphite to graphite, which showed that graphite did inhibit the growth of mesophase formation while $FeCl_3$-graphtie caused an increase in growth, due to the presence of Lewis acid sites.[24] These results point to the importance of acid strength in mesophase growth and coke formation.

Adding water to the reaction medium has also been observed to cause a decrease in coke formation. The use of steam during bitumen pyrolysis by Dutta *et al.* decreased the coke yield up to 4%.[3] Unfortunately, when compared to the dry case, the liquid produced in the presence of steam had a lower H/C ratio, as well as an increased sulfur content.[3] Dutta *et al*. attributed this to the steam stabilizing the reactive aromatic molecules, causing them to remain in the liquid rather than forming coke and resulting in the liquid having a higher H/C ratio and more sulfur.[3] Kirk and Clark noted similar results, where the coke formation is reduced during bitumen pyrolysis in the presence of water.[4] Both studies also noted the constant production of carbon oxides under both wet and dry conditions indicating that any carbon oxides produced were due to oxygen in the feed and not due to water.[3] This implies that hydrogen addition from the water is at most a minor pathway.[4] It is worth noting that these two studies contradict each other in the effect of water on sulfur content with Dutta *et al*.[3] noting an increase in the sulfur content of the liquid, whereas Kirk and Clark[4] noted a decrease in the sulfur content of the liquids.

Finally, the combination of water and solids has also been studied for the upgrading of bitumen and other heavy oils. Kirk and Clark added soluble iron (II) sulfate heptahydrate to water and observed a decrease in the coke yield.[4] They attributed this to the increased ease of electron transfer due to the reduction of Fe^{2+} to Fe^{3+} resulting in the formation of more stable tertiary radicals.[4] In a series of studies using petroleum residues[8-10] and bitumen[11] as feeds, Fumoto *et al*. observed decreases in coke formation when the feed was cracked with ZrO_2-

Al_2O_3-Fe_2O_3. Unlike the previously mentioned studies, Fumoto *et al*. noticed an increase in the formation of carbon dioxide[8,10] as well as the oxygen content of cracked atmospheric residue.[11] They attributed the increased oxygen content to the production of an active oxygen species, produced from the steam over ZrO_2, rather than from the lattice oxygen.[25] Interestingly, Fumoto *et al*. also noted that solely reacting the feed with α-Fe_2O_3 in steam also reduced the coke content, but choose to explore the synthetic catalyst instead.[8]

2.4 The Use of N-Hexadecane as a Model Compound

Understanding the mechanism by which a hydrocarbon decomposes is difficult using a naturally occurring petroleum feed. For this reason, model compounds, such as hexadecane, are employed as a tool to increase our understanding. Although n-alkanes do not occur in bitumen,[17] aliphatic hydrocarbons are often found associated to larger aromatic compounds as branches.[16] Due to the presence of aliphatic side chains, numerous studies have been completed looking at the decomposition of hexadecane and other n-alkanes, both thermally and catalytically.

2.4.1 Gas Phase Pyrolysis of N-Alkanes

The gas phase decomposition of n-hexadecane has been studied extensively. Early work by Rice showed that the initiation step of the decomposition of alkane thermal cracking was the rupturing of a C-C bond and proceeded via a chain reaction propagated by free-radicals.[26] A full mechanism for the early stages of the reaction was later developed,[27, 28] which relied upon the use of Rice's[26] earlier proposal, as is shown in Figure 2-1. This mechanism works well to describe the reaction of the model compound hexadecane at high temperatures, low pressures and low conversions and can be broken down into four reversible steps. The reaction is initiated by the breaking of a C-C bond resulting in the formation of two free radicals. The resulting free radicals then propagate the reaction through steps 2-2 (β-Scission) or 2-3 (H-abstraction). β-Scission relies on the breaking of a bond at the β position to the radical location, while H-abstraction removes hydrogen from another hydrocarbon. It should be noted that although 2-2 and 2-3 are undergoing β-scission and H-abstraction from a primary carbon, the same mechanism would occur at a secondary or tertiary position.

$$R_1 - H_2C - CH_2 - R_2 \longleftrightarrow R_1 - H_2\overset{\bullet}{C} + \overset{\bullet}{C}H_2 - R_2 \tag{2-1}$$

$$R_1 - H_2C - \overset{\bullet}{C}H_2 \longleftrightarrow \overset{\bullet}{R_1} + H_2C = CH_2 \tag{2-2}$$

$$R_1 - H_2\overset{\bullet}{C} + R_1 - H_2C - CH_2 - R_2 \longleftrightarrow R_1 - H_3C + R_1 - H\overset{\bullet}{C} - CH_2 - R_2 \tag{2-3}$$

$$R_1 - H_2\overset{\bullet}{C} + R_1 - H_2\overset{\bullet}{C} \longleftrightarrow R_1 - H_2C - CH_2 - R_2 \tag{2-4}$$

Figure 2-1. Rice-Kossiakoff mechanism for alkane decomposition[27, 28]

The effects of temperature, pressure, residence time and dilution have all been studied extensively for this reaction. As can be seen from steps 2-2 to 2-4, the gas phase of decomposition of alkanes is greatly impacted by the pressure of the reactor. Voge and Good[29] demonstrated that, at lower pressure, all the linear alkenes and alkanes from methane to tetradecane were produced, but the primary hydrocarbon product was C_4 or lighter and had a high alkene content. Voge and Good[29] then increased the pressure, resulting in a decreased yield of products lighter than C_4, and a decreased alkene content. This is expected because as the pressure increases the probability of 2-3 and 2-4 occurring greatly increases, because of the increased concentration of possible reactants. Therefore, 2-2 is less important, explaining the decreased olefin content, as well as the yield of light hydrocarbons. Similar results have also been seen where by increasing the amount of steam or argon effectively lowered the partial pressure of hexadecane and led to an increased yield of light hydrocarbons and specifically alkenes.[30,31] In addition to pressure, temperature is also known to significantly affect the product distribution for gas phase cracking.

Temperature impacts both the rate of the reaction as well as the resulting product distribution. The activation energy for the initiation of hexadecane cracking has been reported to be 75 kcal/mol,[32] while the overall activation energy is only 57 kcal/mol.[33] This is important to note because as the temperature increases, so does the rate of cracking of the hexadecane molecule, causing a change in the product distribution due to the increased ability to crack the parent hydrocarbon (2-1) as well as any radicals (2-3).[32] In general, increasing the temperature of cracking results in a shift to lighter hydrocarbons with a high alkene content.[30, 34] Furthermore, temperature also effects the probability of H-abstraction and β-Scission occurring. As Safarik and Strausz[35] discussed, H-abstraction has an activation energy approximately 20 kcal/mol lower than β-Scission, meaning that, at lower temperatures, the probability of H-abstraction is increased compared to β-Scission, leading to a heavier overall product. Finally, Depeyre *et al.*[30] noticed that hydrogen production increased as the temperature increased, as would be predicted given the higher bond dissociation energy of the C-H bond compared to a C-C bond.

2.4.2 Liquid Phase Pyrolysis of N-Alkanes

The Rice-Kossiakoff mechanism has been shown to work quite well at low pressures, high temperatures and low conversions. As the pressure inside the reaction vessel is increased, however, and the predominant cracking medium is in the liquid phase, this mechanism begins to falter. Although the rate constants and activation energies for the degradation of n-hexadecane are nearly identical for the gas and liquid phase cracking, it has been noticed that the product distribution changes drastically.[33,34,36] These changes include a decrease in gas formed ($<C_5$), an increase in the alkane to alkene ratio and the formation of higher molecular weight products. These phenomena have been attributed to bimolecular reactions occurring within the liquid phase,[33, 36] as expected due to the increased density of molecules available to react with a free radical.[37] Examples of these bimolecular reactions can be seen in Figure 2-2. Wu *et al.*[34] completed a study comparing the decomposition of hexadecane at the same temperature in the gas and liquid phase and noted a decrease in the production of C_4 or lighter when cracked in the liquid phase, indicating that the β-Scission propagation step is being hindered. Similar

results were observed by Ford, who noticed that at conversions less than 1%, 1 mole of alkenes and 1 mole of alkane is formed from 1 mole of hexadecane.[33] Both of these results are attributed to the fact that produced alkyl radicals have an increased probability of abstracting hydrogen from hexadecane to produce a hexadecyl radical (2-5). To test the impact of hydrogen abstraction on hexadecane decomposition, Khorasheh and Gray[38] used a 5% concentration of hexadecane in benzene. By using benzene as a solvent they were able to effectively reduce the number of abstractable hydrogen's which caused the reaction selectivity of the n-alkanes to shift to a lower carbon number, while simultaneously increasing the selectivity for olefins.[38]

$$\dot{R} + C_{16}H_{34} \longleftrightarrow RH + \dot{C}_{16}H_{33} \tag{2-5}$$

$$\dot{R}_1 + H_2C = CH - R_2 \longleftrightarrow R_1 - H_2C - \dot{C}H - R_2 \tag{2-6}$$

Figure 2-2. Bimolecular reactions occurring during the liquid phase n-alkane cracking

As the reaction continues to propagate and conversion increases, Ford[33] observed the formation of high molecular weight compounds and a decrease in the alkene content. By cracking hexadecane and 1-decene in the liquid phase, Ford[33] observed all the linear alkanes and alkenes as well as a large amount of C_{26} alkanes. The formation of C_{26} alkanes is indicative of the reaction of hexadecyl radicals with 1-decene via reaction 2-6, with further evidence of the addition reaction being the appearance of 8 peaks for each carbon number from C_{18} to C_{30} at any of the 8 unique locations on the hexadecane backbone.[33] As mentioned, Khorasheh and Gray[38] cracked hexadecane in benzene to reduce the probability of H-abstraction occurring. By changing the solvent to toluene, Khorasheh and Gray[38] created a system which H-Abstraction can happen more readily due to the decreased C-H bond energy (Table 2-2). As expected, the change in solvent increased the selectivity for higher carbon number alkanes, while also yielding a significant amount of alkylbenzenes, proving that within the liquid phase, radicals are capable of reacting with alkenes to produce larger hydrocarbons.[38] Therefore, the mechanism proposed for the gas-phase only applies to the liquid-phase at low conversions. As the conversion and subsequently the alkene concentration increases, so to does the probability of bimolecular addition reactions occurring.

Table 2-2. Bond dissociation energies of 6 types of C-H bonds found in the reaction system[39]

Bond	Bond dissociation energy (kcal/mol)
CH_4	101.1
CH_3-CH_2-H	98.6
$(CH_3)_2$-CH-H	96.5
$(CH_3)_3$-C-H	104.99
C_6H_5-H	112.9
C_6H_5-CH_2-H	89.8

As mentioned, n-alkanes do not exist within bitumen.[17] The only saturated aliphatic groups exist as branches of larger aromatic compounds.[16] Although these aliphatic groups follow the same mechanism as that of n-alkanes, there are a few key differences. As Savage *et al.*[40] demonstrated, all n-alkanes, 1-alkenes, phenylalkanes and phenylalkenes are produced, but the main products from the decomposition of pentadecylbenzene are toluene, 1-tetradecene, styrene and n-tridecane. The change in the product distribution results from the addition of the aromatic group to the alkyl chain, which favors β-scission either beginning with or resulting in a more stable benzyl radical.[37] Therefore, as Savage *et al.* showed, β-scission is favored when the radical is initially located on either the α or γ carbons.[40] Interestingly, at low concentrations, the cracking of 1-dodecylpyrene follows the same pathway and results in the formation of methylpyrene, 1-undecene, vinylpyrene, ethylpyrene and n-decane.[41] However, at high concentration, the product distribution changes to form n-dodecane and pyrene, which Smith and Savage attribute to selective hydrogenolysis of the pyrene ring resulting in the cleavage of the dodecane side chain.[41] Thus, when existing as an alkyl side chain, alkane groups will crack following the mechanism suggested for n-alkanes. However, they will favor a pathway that results in the formation of a radical capable of undergoing resonance stabilization.

2.4.3 Catalytic Cracking of N-Alkanes

Unlike the liquid and gas phase thermal cracking, the catalytic cracking of n-alkanes has been studied significantly less extensively, resulting in a mechanism that has produced a significant amount of discontent. The main source of discontent revolves around the initiation of n-alkane cracking.[42] Figure 2-3, displays the proposed mechanism for the initiation of catalytic n-alkane cracking. It has been proposed that initiation requires the presence of an alkene (2-7) which can be protonated to form a carbenium ion capable of propagating the reaction.[43] It has also been proposed that the initiation follows the Haag-Dessau mechanism, which calls for the protonation of an alkane by a solid acid to produce a carbonium ion which will decompose to leave a carbenium ion and an alkane (2-8).[44] Finally it has been proposed that it is possible that the reaction may be initiated by the abstraction of a hydride ion (2-9).[42]

$$C_nH_{2n} + H^+ \longleftrightarrow C_nH^+_{2n+1} \tag{2-7}$$

$$C_nH_{2(n+1)} + H^+ \longleftrightarrow C_nH^+_{2(n+1)+1} \longrightarrow C_iH_{2(i+1)} + C_{n-i}H^+_{2((n-i)+1)-1} \tag{2-8}$$

$$C_nH_{2(n+1)} + L^+ \longleftrightarrow C_nH^+_{2(n+1)-1} + L^+H^- \tag{2-9}$$

Figure 2-3. Proposed initiation reactions for catalytic cracking of alkanes

Contrary to initiation, propagation is agreed upon and known to occur through a carbenium ion on the surface of the catalyst.[42] Figure 2-4 displays the mechanism by which the cracking of alkanes will proceed regardless of the initiation. The carbenium ion can be desorbed from the surface by abstracting a hydride ion from another alkane[42], which at low conversions is expected to be the parent alkane, resulting in the production of an alkane and the parent carbenium ion on the catalyst surface (2-10). Furthermore, any carbenium ion on the surface can also undergo β-Scission resulting in the formation of an alkene and a smaller carbocation which can propagate the reaction (2-11).[42] This monomolecular reaction will, much like thermal cracking, result in the production of an alkane to alkene ratio of 1,[45] with the alkane produced following the absraction of a hydride ion and subsequent desorption. However, catalytic cracking often results in an alkane to alkene ratio greater than 1, due to disproportionation and oligomerization reactions.[45-47] Disproportionation reactions have been observed from the catalytic cracking of isobutene[45] and isopentane[46]. Disproportionation occurs when a carbocation reacts with an alkane to produce a large carbonium ion which can then undergo cracking to produce an alkane while leaving behind a carbenium ion (2-12).[46] Finally, the carbocation may also react with an alkene to produce a larger carbenium ion which can undergo any of reactions 2-10 to 2-12 to produce a larger alkene or alkane.[47] The reaction is ultimately terminated by the desorption of the carbenium ion to regenerate the Bronsted acid site and produce an alkene.[42]

$$S^{-}[C_nH_{2(n+1)-1}]^{+} + C_{16}H_{34} \longleftrightarrow S^{-}[C_{16}H_{33}]^{+} + C_nH_{2(n+1)} \tag{2-10}$$

$$S^{-}[C_nH_{2(n+1)-1}]^{+} \longleftrightarrow S^{-}[C_{n-i}H_{2((n-i)+1)-1}]^{+} + C_iH_{2i} \tag{2-11}$$

$$S^{-}[C_nH_{2(n+1)-1}]^{+} + C_{16}H_{34} \longleftrightarrow S^{-}[C_{16+n}H_{2n+35}]^{+} \tag{2-12a}$$

$$S^{-}[C_{16+n}H_{2n+35}]^{+} \longrightarrow C_iH_{2(i+1)} + S^{-}[C_{16+n-i}H_{2(n-i)+33}]^{+} \tag{2-12b}$$

$$S^{-}[C_nH_{2(n+1)-1}]^{+} + C_iH_{2i} \longleftrightarrow S^{-}[C_{n+i}H_{2(n+i+1)-1}]^{+} \tag{2-13}$$

$$S^{-}[C_nH_{2(n+1)-1}]^{+} \longleftrightarrow S^{-}H^{+} + C_nH_{2n} \tag{2-14}$$

Figure 2-4. Propagation and termination reactions for the catalytic cracking of alkanes. (S=Heterogeneous catalyst)

2.5 The Use of α-Fe_2O_3 as a Catalyst and Reactant

Catalytic cracking relies upon the use of Bronsted and Lewis acid sites, both of which are found on the surface of α-Fe_2O_3.[48] α-Fe_2O_3 (hematite), is a thermally stable, naturally occurring iron oxide with a hexagonally close-packed structure similar to that of corundum (Al_2O_3).[49] Industrially, the use of α-Fe_2O_3 has been explored for a number of processes including styrene production,[49] water-gas shift reactions,[49] Fischer-Tropsch synthesis[49] and gas scrubbing.[50] Unlike the hydroxides such as goethite (α-FeOOH), α-Fe_2O_3 contains no structural hydrogen. This means that, under dry conditions, α-Fe_2O_3 is coordinately unsaturated.[51] In the presence of water, however, the surface becomes saturated with hydroxyl groups.[49] At ambient pressure and temperature, it has been observed that water adsorbs onto the surface and dissociates to produce surface hydroxyl groups (Figure 2-5).[52] As Ferretto *et al.*[48] demonstrated, hydroxyl groups are capable of acting as a Bronsted acid, and are therefore being explored as potential catalyst for catalytic cracking.

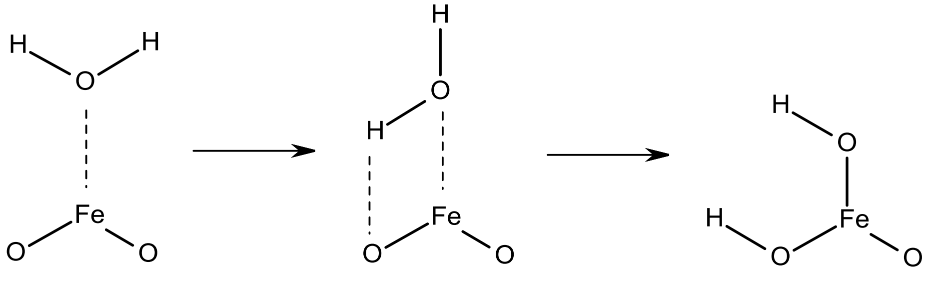

Figure 2-5. Dissociation of water on the unsaturated surface of α-Fe_2O_3 to produce surface hydroxyl groups (Adapted from Yin, 2007)[53]

As mentioned, under dry conditions[51] or at high temperatures[54] a fraction of the α-Fe_2O_3 surface is coordinately unsaturated. This unsaturation produces a surface containing unsaturated metal cations capable of acting as Lewis acids.[51] These sites are then free to interact with any compounds capable of donating their electrons, including H_2, CO, H_2O, H_2S and alkenes.[51] Water may donate the lone pair of electrons on its oxygen to the metal cation and dissociatively adsorb to produce a hydroxylated surface or it may non-dissociatively adsorb (or molecularly adsorb) on the surface.[53] Similarly, alkenes and aromatics may also adsorb via their π-bonds. Dent and Kokes studied the adsorption of propene and ethylene on the surface of ZnO and found that they can dissociate.[55] In addition, Busca *et al*. observed that hydrocarbons such as ethylene and benzene can also be combusted after adsorbing through their π-bonds.[56, 57]

In addition to the Lewis and Bronsted acidity of α-Fe_2O_3, it can also oxidize hydrocarbons, resulting in the reduction of α-Fe_2O_3 to Fe_3O_4 (magnetite).[58, 59] The reduction of metal oxides, such as α-Fe_2O_3, and subsequent oxidation of the hydrocarbons to produce water and the carbon oxides is thought to proceed via the Mars-Van Krevelen Mechanism.[60] At temperatures less than 420 °C and under severe reducing conditions, (i.e. $\frac{H_2}{H_2+H_2O} > 0.8$ or $\frac{CO}{CO+CO_2} > 0.45$), Fe_3O_4 can reduce directly to Fe.[61] Conversely, under oxidizing conditions (in the presence of oxygen or steam), metallic iron can be oxidized into Fe_3O_4.[62] However, only oxygen can oxidize Fe_3O_4 to Fe_2O_3 as it is thermodynamically impossible for this reaction to proceed using steam.[62, 63] Finally, iron oxides such as α-Fe_2O_3 are capable of interacting with H_2S to produce iron sulfides.

During the steam cracking of coal derived liquids with α-Fe_2O_3, Sharypov *et al*. observed the formation of pyrrhotite and a reduction in H_2S indicating that the iron oxide was adsorbing the H_2S.[64] Davydov *et al*.[65] explained that the H_2S acts as a Lewis base on the unsaturated surface and is dissociatively adsorbed (similar to Figure 2-5), followed by the immediate rearrangement to yield water. Similar results have also been noticed in the presence of hydrogen during the cleaning of coal derived gas with natural and synthetic α-Fe_2O_3[13], as well as during coal liquefaction with α-$Fe_2O_{3.}$[12] Contrary to Fe_3O_4, iron sulfides are capable of being oxidized by steam. During coal pyrolysis in the presence of steam, it was observed that at temperatures greater than 350°C pyrite (FeS_2) was oxidized to Fe_3O_4 and Fe_2O_3.[66]

2.6 The Decomposition of Sulfur Containing Compounds

Given that α-Fe_2O_3 can react with compounds such as H_2S, it is important to discuss the decomposition of some heteroatom compounds found in bitumen. As previously mentioned, bitumen contains approximately 4.5% sulfur, 1.1% oxygen and 0.4% nitrogen[16], however, for the sake of this study only sulfur compounds will be discussed. The sulfur within the bitumen is present within two main classes of compounds: sulfides and aromatic rings, as shown in Figure 2-6. It has been estimated that sulfides make up between 26%[67] and 38%[68] of the total sulfur. Greinke *et al*. showed that sulfur in aliphatic chains is highly labile, while sulfur within aromatic rings, such a dibenzothiophene, is stabilized resulting in negligible decomposition at temperatures less than 800 °C.[69] Due to the fact that upwards of 62% of the total sulfur is found in aromatic rings, it is not surprising that the majority of sulfur is found heavier fractions[67] with the majority ending up within the insoluble during coking.

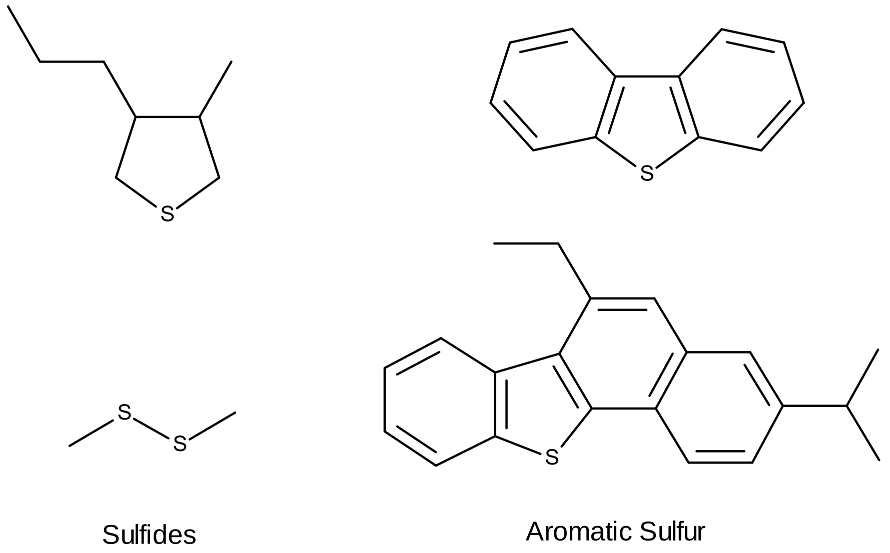

Figure 2-6. Representative compounds depicting structure of sulfur in bitumen

During the coking process, sulfides break down to form hydrogen sulfide through a free radical chain mechanism[37] similar to that shown for decomposition of the n-alkanes. Based on the structure of dimethyl disulfide (Figure 2-6), the decomposition may be initiated by a C-S, S-S or C-H bond breakage. However, the C-H bond energy is found to be a minimum of 100 kJ/mol higher than the S-S (270.5 kJ/mol) or C-S (236.8 kJ/mol) bonds,[70] indicating that the most plausible initiation is through the cracking of a C-S or S-S bonds.[71, 72] When performed in the liquid phase the sulfide radicals can abstract a hydrogen from a neighboring hydrocarbon,[37] resulting in the formation of a radical and saturated compounds.

Depending on the nature of the compound, the reaction may be further propagated by the breaking of other C-S or S-S bonds until the subsequent formation of H_2S.[37, 71] For this example (Figure 2-7) dimethyl disulfide was chosen as it is used during the experimental study. However it should be noted that had a larger alkyl sulfide been chosen, β-Scission would have also occurred. Furthermore, numerous other reactions could also occur during the decomposition of dimethyl disulfide,[70] however, only those reaction leading to the formation of hydrogen sulfide are considered here.

Initiation

$$H_3C-S-S-CH_3 \longleftrightarrow H_3C-\dot{S}+\dot{S}-CH_3$$

$$H_3C-S-S-CH_3 \longleftrightarrow H_3\dot{C}+\dot{S}-S-CH_3$$

Propagation

$$\dot{S}-CH_3+RH \longleftrightarrow HS-CH_3+\dot{R}$$

$$HS-CH_3 \longleftrightarrow H\dot{S}+\dot{C}H_3$$

$$RH+H\dot{S} \longleftrightarrow H_2S+\dot{R}$$

Termination

$$\dot{R}+\dot{R} \longleftrightarrow R-R$$

Figure 2-7. Decomposition of dimethyl disulfide to produce hydrogen sulfide (Adapted based on the work of Gray and McCaffrey)[37]

Based on the previously stated information and the fact that Fumoto *et al.*[8] noticed a decrease in the coke yield during the cracking of residue in the presence of steam and α-Fe_2O_3, the objectives of this study will be to examine the simultaneous use of α-Fe_2O_3 and steam as a method of catalytically cracking bitumen while decreasing the coke yield of bitumen and increasing its sulfur content.

Chapter 3: Materials and Methods

3.1 Procedure

3.1.1 General Reaction Information

All reactions were performed in the liquid phase using 15 mL stainless steel batch reactors assembled using swagelock fittings. Reactions were completed within a Tacam SBS-4 fluidized sand bath. Figure 3-1 shows a schematic representation of the reactor set-up used. Typically 1/8” stainless steel (SS) tubing is employed, however, these reactions required an agitation speed of 350 rpm rather than 175 rpm and therefore ¼” SS tubing with a 0.35” wall was used to prevent the tubing from bending or breaking. A ¼” SS integral bonnet needle valve was attached to the tubing to allow pressurization of the reactor. The valve was also directly attached to a steel plate with a 2.5 cm diameter hole used to attach the apparatus directly to the agitator. The steel plate was two separate pieces joined by hex key bolts, allowing for the plate to be added and removed from the agitator.

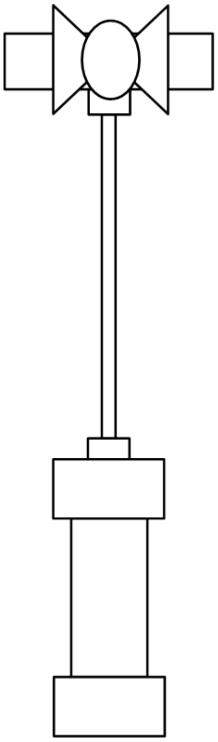

Figure 3-1. 15 mL SS microbatch reactor schematic

The agitator consisted of a 6 cm diameter cam attached directly to a 5:1 gear reducer to produce a rotation of 350 rpm. A rear end bearing was attached to a 36 cm long, 2.5 cm diameter steel rod and attached to the cam at a 1 cm offset. Given that the sand bath was of a set height, it was required that the length of reactor tubing be 7” long to ensure the reactor is continuously within the sand. Figure 3-2 provides a schematic representation for the agitator setup.

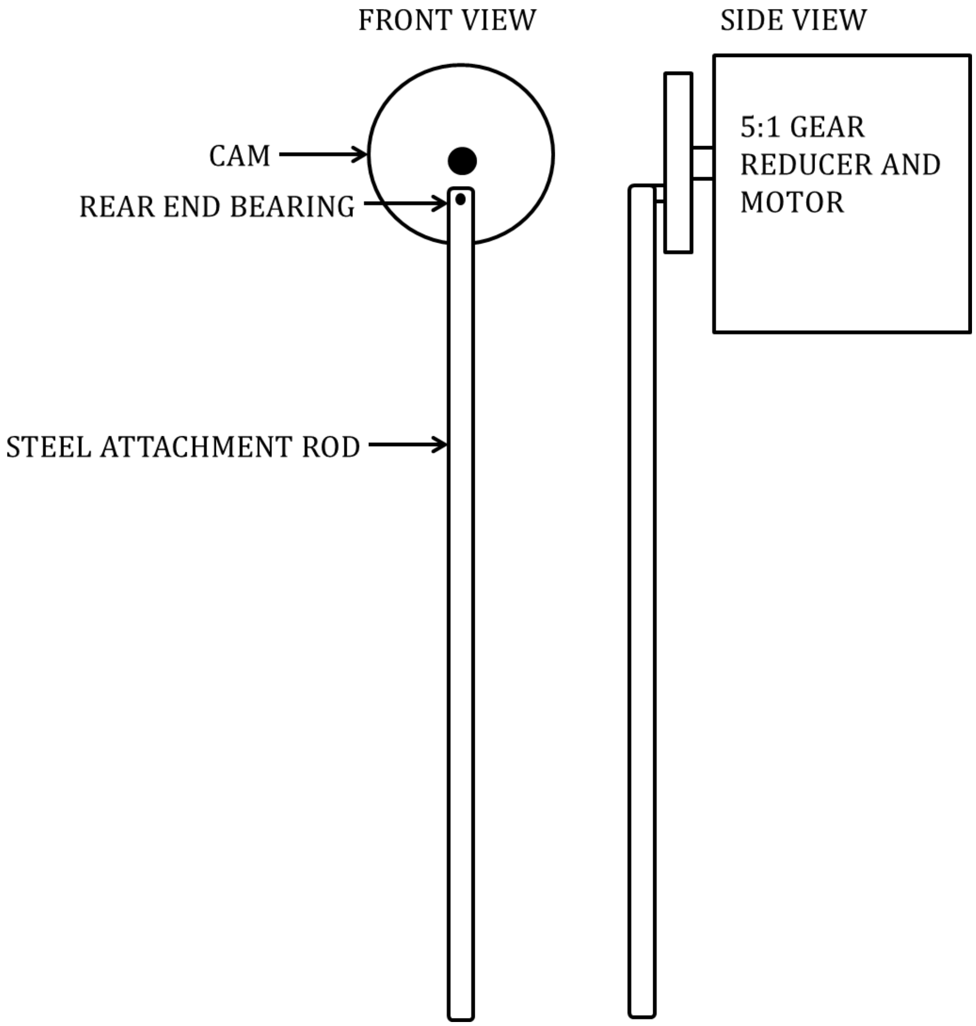

Figure 3-2 Schematic of agitator used to provide agitation at 350 rpm

For each reaction the sand bath was given a set-point of 420 °C. Figure 3-3 displays the internal reactor temperature as a function of time with a set point of 420 °C. The internal temperature was measured using a k-type thermocouple and compared to a k-type thermocouple inserted directly into the sand bath. The internal reactor temperature reaches 415 °C within approximately 3 to 4 minutes of being placed in the sand bath. This is important as it implies that the heat up time accounts for less than 10% of the total residence time for a reaction of 45 minutes. The reactor was cooled by exposing it to a continuous stream of cool air, which, as shown in Figure 3-3, brought the reactor below 200 °C within 4 minutes. It was observed that, depending upon the location of the external thermocouple, the temperature of the sand bath could vary by as much as 5 °C. To account for this, each reaction was attempted to be placed in the same location within the sand bath. It is also expected that the temperature of the sand bath would vary slightly each day. Therefore, no two duplicate reactions were performed back-to-back to minimize the error incurred by instability in the sand bath between days. Within this document, all temperatures referenced are those of the set point because the temperature of the reaction could not be measured for each reaction.

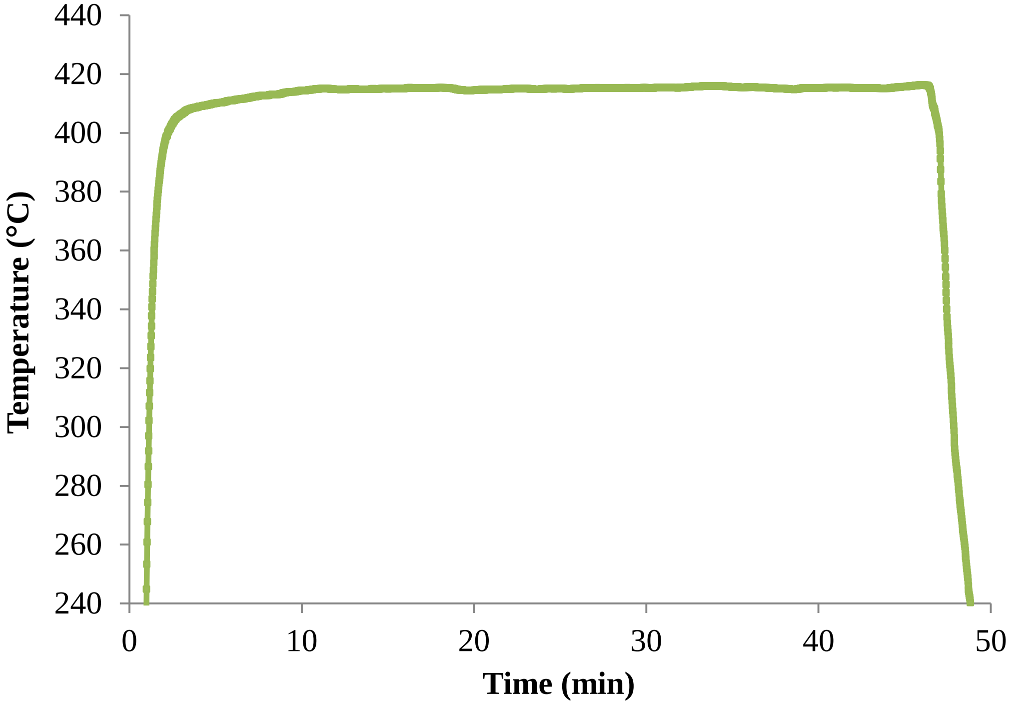

Figure 3-3. Internal reactor temperature as a function of time for a reaction with a sand bath set-point of 420 °C

3.1.2 Hexadecane Cracking

For each reaction, 3 g of 99% hexadecane obtained from Sigma-Aldrich was accurately weighed into a batch reactor. The effect of α-Fe_2O_3 on the liquid phase cracking of hexadecane was studied by adding 0-10%wt of 99+% <5 µm Iron(III)Oxide as supplied by Sigma-Aldrich. The effect of water was tested by adding 0-10%wt reverse osmosis (RO) water. Finally, 3 SS balls were added to aid in mixing. After adding all required components, the reactor was sealed and pressurized to 5000 kPa using nitrogen, and leak tested using Snoop® liquid leak detector. The formation of any bubbles within the Snoop® resulted in the reactor being declared to have a leak and re-opened and subsequently re-sealed and leak tested again. This was repeated until no leaks were detected. Having completely sealed the reactor, nitrogen was used to purge the reactor of oxygen by filling and releasing the nitrogen five times using the initial reactor pressure. After purging five times, the reactor was sealed at the initial reaction pressure. The initial closed pressure was chosen to be 2500 kPa in the absence of water. Initial vapour-liquid equilibrium calculations showed that at 420 °C a pressure of greater than 992 kPa was required to ensure the hexadecane was in the liquid phase. During the reactions that included water, the initial reactor pressure was lowered to 1000 kPa to account for the partial pressure of water. The pressure of the reactor was chosen such that when 5 %wt water was added the total pressure would be approximately equal for both cases. Prior to and after closing the reactor, the reaction apparatus was weighed to measure the mass of nitrogen added to the reactor as part of the mass balance.

The cracking of hexadecane was completed at 420 °C for 45 minutes in a sand bath. Upon completion, the reactor was air cooled to room temperature and then placed in a freezer overnight. Freezing was used to limit the loss of heavier materials being carried out by the released gases and to decrease the standard deviation of the produced gases by ensuring the same internal temperature for each reactor when opened. After freezing, the gaseous phase was slowly released into a 500 mL SKC quality sample bag for analysis via gas chromatography. Prior to and after releasing the gases, the reaction apparatus was weighed to determine the amount of gaseous products produced from the cracking. The mass of the gas was calculated using 3-1, 3-2 and 3-3.

$$m_{R,apparatus,N2} - m_{R,apparatus} = m_{N2} \tag{3-1}$$

$$m_{R+Gases} - m_{R-Gases} = m_{Gases} \tag{3-2}$$

$$m_{Gases} - m_{N2} = m_{Gas\,\mathrm{Pr}oduced} \tag{3-3}$$

After weighing the reaction apparatus, the tubing and bracket were removed and the reactor was again weighed to determine the mass of the reactor containing the solid and liquid products. The liquid products were removed using a pasteur pipet and transferred into a sample vial. The solids were removed from the reactor using ACS certified Methylene Chloride from Fischer Scientific and separated using a Durapore® 0.22 μm PVDF membrane filter and dried at 70 °C for 1 hour. Having removed both the liquid and solid the reactor was again weighed to determine the mass of the liquid and the solid (3-4). The final mass of the liquid was measured by removing the mass of α-Fe_2O_3 initially added (3-5). Although α-Fe_2O_3 will be reduced to Fe_3O_4, this only corresponds to a 3.3% mass loss, which was ignored as full reduction was never observed and thus is negligible. Prior to analyzing the liquid via gas chromatography, anhydrous magnesium sulfate ($MgSO_4$)[4] from Fischer Scientific was added to remove any non-reacted water and centrifuged for 7 minutes at 7000 rpm to remove the $MgSO_4$ and any other solid particles. Each hexadecane reaction was completed in quadruplicate.

$$m_{R+Solids+Liquid} - m_R = m_{Solids+Liquid} \tag{3-4}$$

$$m_{Solids+Liquid} - m_{Fe} = m_{Liquid} \tag{3-5}$$

A separate study was performed using the same procedure as above but with the inclusion of 99.0% Methyl Disulfide from Sigma-Aldrich. A stock solution containing hexadecane and dimethyl disulfide was produced containing 3300 ppm of sulfur. Another study was also completed using Ferrous Sulfide from Fischer Scientific rather than Iron(III)Oxide, but again used the identical procedure.

3.1.3 Cold Lake Bitumen Cracking

The impact of water and α-Fe_2O_3 on the cracking of bitumen was investigated using Cold Lake bitumen. The elemental composition of the main constituents of Cold Lake bitumen can be seen in Table 3-1. Cold lake bitumen was chosen as the feed since it contains less than 1% solids. Three grams of bitumen, 0-20%wt RO water, 0-10%wt α-Fe_2O_3 and 3 stainless steel balls were accurately weighed and added to the reactor. The reactor was pressure tested in a method identical to hexadecane but instead up to a pressure of 12 MPa. After pressure testing, the reactor was again purged five times with nitrogen, but now closed at 101 kPa and 5000 kPa in the presence and absence of water, respectively. Similar to that of hexadecane, the mass of nitrogen was measured before the reaction to aid in the determination of the amount of gas produced (3-1 to 3-3).

Table 3-1 Elemental composition of Cold Lake bitumen

Element	wt%
Nitrogen	0.94
Carbon	83.21
Hydrogen	9.15
Sulfur	5.16
Oxygen (by difference)	1.54

The bitumen was cracked at 420 °C for 60 and 120 minutes. After cracking, the reactor was air-cooled to room temperature. The mass of the produced gas was measured by weighing the reaction apparatus prior to and after releasing the gas into a gas bag, which was subsequently analyzed by gas chromatography. After removal of the gas, the reaction apparatus was disassembled and the mass of the reactor without the tubing was measured to determine the mass of the reactor plus that of the liquids and solids. The liquid and solid products were extracted from the reactor using a 40:1 ratio of toluene to feed and transferred into a 250 mL beaker. The walls of the reactor were scraped to remove any adhered coke using a steel brush. After extracting all of the material, the reactor was dried at 120 °C before being weighed to determine the mass of liquid and solids in the reactor.

The extracted material was then mixed for 15 minutes using ultrasonic dispersion to ensure the entire liquid product was dissolved in the toluene. The coke (toluene insoluble) and catalyst were separated from the liquid product by filtering with a Durapore® 0.22 μm PVDF membrane filter. The solids were continually washed with toluene until the resulting filtrate was clear, indicating all of the liquid product had been removed. The separated solids were then dried in a vacuum oven at 70 °C for 12 hours. The mass of the resulting coke was measured and subtracted from the mass of the liquid and solid products inside the reactor to determine the yield of the liquid product (3-6, 3-7 and 3-8). The liquid filtrate was separated into a toluene fraction and a heavier organic fraction using rotary evaporation at 60 °C and 77 mbar for 2 hours.

$$m_{filter+solids} - m_{filter} = m_{solids} \tag{3-6}$$

$$m_{solids} - m_{Fe} = m_{coke} \tag{3-7}$$

$$m_{liquid+solids} - m_{solids} = m_{liquid} \tag{3-8}$$

3.1.4 Agitation

Initially, the reactor was agitated at 175 rpm, however, this was found to provide inadequate mixing and a second agitator was designed with an agitation speed of 350 rpm. To prove that the agitation rate was insufficient, a replica acrylic reactor was constructed to allow for qualitative observations of the mixing. Although hydrocarbons are used in the cracking experiments, water was employed as the liquid phase to prevent the hydrocarbons from dissolving the acrylic reactor. It was also decided that Fe_3O_4 would be used as the solid given that it has less oxygen and should therefore interact less with the water and provide a system, which more closely mimics that under reaction conditions. Agitation of this system at 175 rpm showed that the liquid level did not move and the solid catalyst sat at the bottom of the reactor throughout agitation. This implies that the only interaction between the catalyst and gaseous atmosphere would be through the gases dissolved in the liquid. On the other hand, when agitation was provided at 350 rpm the liquid level continually moved and filled the entire reactor, allowing for sufficient interaction between the gas and liquid phases. The liquid phase was entirely black implying that solid was well dispersed and able to interact sufficiently with the other two phases. These results were later confirmed by cracking hexadecane at 420 °C for 45 minutes with 5%wt water as can be seen by Figure 3-4. This figure shows that when the reactor is agitated at 175 rpm the α-Fe_2O_3 comes out black indicating a reduction to Fe_3O_4, however, when the agitation is set to 350 rpm the catalyst comes out dark red indicating that the steam was in fact interacting with the catalyst resulting in a catalyst that more closely resembles α-Fe_2O_3.

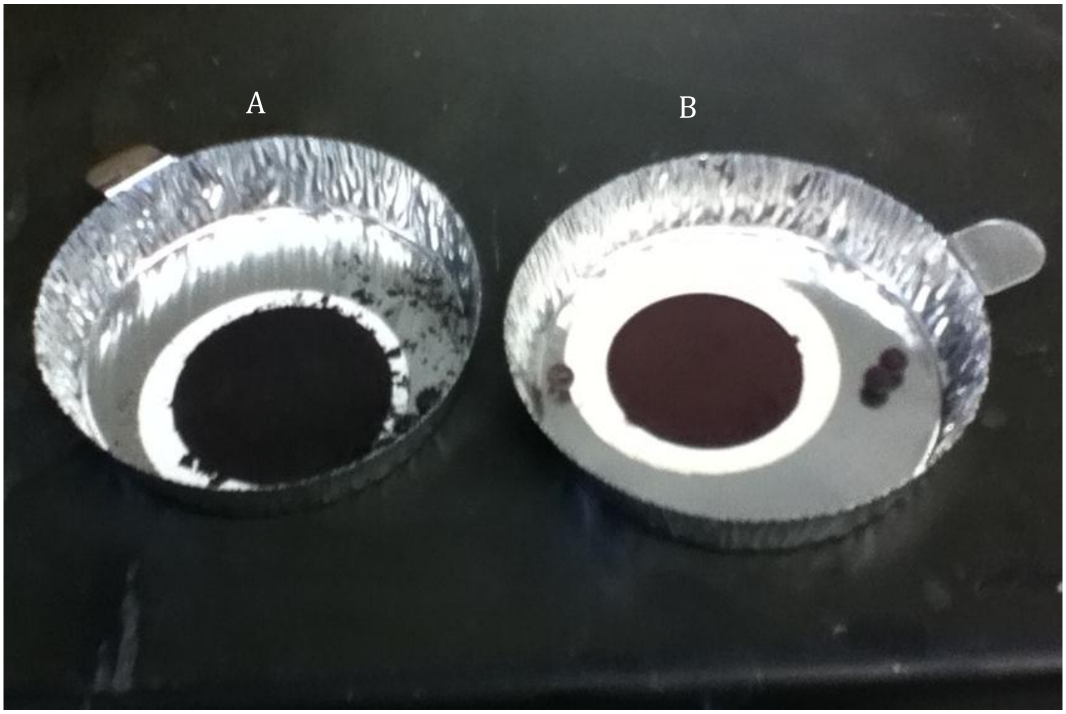

Figure 3-4. Solid catalyst following the cracking of hexadecane with an agitation rate of a) 175 rpm and b) 350 rpm

3.2 Analytical Analysis

3.2.1 Liquid Injection Gas Chromatography

The liquid products produced from the cracking of hexadecane were quantified using an Agilent 7890A GC. Gas Chromatography (GC) is capable of quantifying the hydrocarbons present in a sample based on their response factor to a given detector. Quantification was completed using a flame ionization detector at 300 °C and nitrogen as the carrier gas. For each run 0.2 μL of sample were injected thru the inlet at 250 °C with a split ratio of 130:1. Separation was completed using a 50 m Agilent HP PONA column with a 200 μm I.D and a 0.5

μm thick film. The initial column temperature was set to 35 °C and heated at 5 °C/min to 230 °C followed by heating at 10 °C/min to 310 °C. The column was kept at 310 °C for 12 minutes at which point all compounds had eluted.

Methylcyclohexane (99% extra pure) from Agros Organics was used as an internal standard. Each day a minimum of 4 standards were run to produce a response factor for methylcyclohexane to hexadecane. The response factor of hexadecane to all other hydrocarbons was assumed to be 1 based on previous literature.[73] A new calibration curve was run each day as the response of the GC was shown to change slightly from day to day. The resulting response factors ranged from 1.158 to 1.287, all with R^2 values greater than 0.99743. Quantification was completed by accurately weighing 0.5 g of the produced liquid and 0.5 g of methylcyclohexane into a sampling vial. The concentration of hexadecane was determined using equation 3-9 where R_f is the response factor calculated through calibration.

$$\frac{m_{Hexadecane}}{m_{Methylcyclohexane}} = R_f \frac{A_{Hexadecane}}{A_{Methylcyclohexane}} \tag{3-9}$$

3.2.2 Gas Injection Gas Chromatography

The produced gas from both the hexadecane and bitumen cracking was analyzed using an Agilent 7890A GC with a helium carrier gas. This separate setup allowed for samples to be injected from a 500 mL SKC gas bag. The gas bag was compressed for a minimum of 20 seconds to allow for the gases to completely fill the inlet valve. After 20 seconds the run was started and the injection valve (V1) was switched to inject the sample into the column. To allow for sufficient separation two columns in series were employed. Figure 3-5 displays the set-up of the valves, columns and detectors used. The first column is a 10’ x 0.125” O.D. HayeSep R column with an 80/100 mesh, while the second column is a 10’ x 0.125” O.D. 13X Molecular sieve column. The initial oven temperature is held at 70 °C for 7 minutes and then heated at 10 °C/min to 250 °C before being cooled at 30 °C/min to 70 °C and held for 8 minutes. After 1.75 minutes, valve 2 (V2) is closed, at which point H_2, N_2, CO and Argon have passed through column 1 and are enclosed within column 2. The remaining compounds are then free to traverse into a parallel line and into a thermal conductivity detector and then a flame ionization detector. This set-up is used to prevent the hydrocarbons from entering the molecular sieve and from permanently contaminating the column. After 34 minutes, valve 2 is switched again resulting in column 2 becoming part of the circuit and the remaining compounds being separated and swept out by the carrier gas.

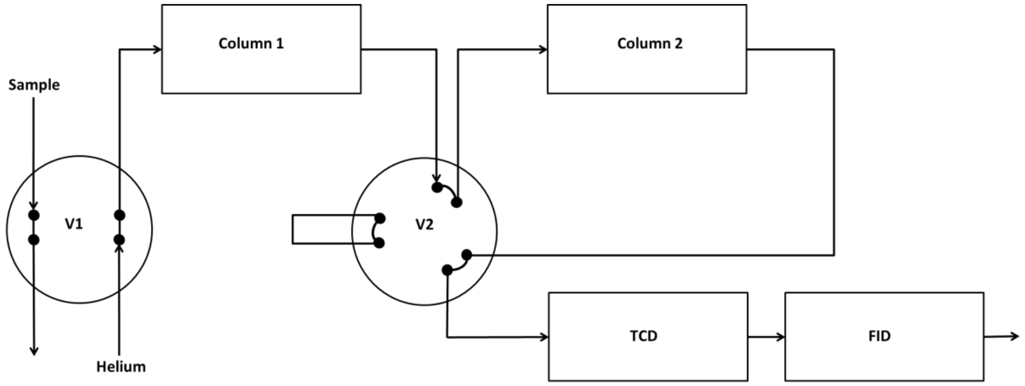

Figure 3-5 Schematic representation of gas phase GC separation

3.2.3 Gas Chromatography – Mass Spectrometry (GC-MS)

The products from the cracking of hexadecane were identified using a Thermoscientific Trace GC Ultra coupled with a DSQII mass spectrometer. A microsyringe was used to inject a 1 µL sample containing approximately 95% of ACS certified Methylene Chloride with the remainder consisting of the analyzed sample. The sample was injected through an inlet held at 250 ˚C with a 50:50 split. The sample was carried through the instrument by a nitrogen carrier gas at a flow rate of 1 mL/min. Compounds were separated within the GC using a 30 m TR-5MS with an ID of 0.25 mm and a film thickness of 0.25 µm. The column was initially maintained at 40 ˚C for 5 minutes followed by heating at 6 ˚C/min to 300 ˚C and held isothermally for 10 minutes. The separated products were transferred to the DSQII MS through the MS transfer line at 300 ˚C to prevent condensation. The MS was turned on 2 minutes after injection to prevent the detector from being overloaded by the solvent. The resulting chromatogram and mass spectrum was analyzed using XCalibur software and the provided library along with the NIST library.

3.2.4 X-Ray Diffraction

X-Ray Diffraction (XRD) was used to distinguish between the hematite crystal structure (α-Fe_2O_3) and the magnetite crystal structure (Fe_3O_4). During the reaction the H_2, CO_2, CH_4 and various other hydrocarbons can cause the reduction of α-Fe_2O_3 to Fe_3O_4. XRD analysis was performed by trained technician at the

University of Alberta using a Rigaku Ultima IV unit with a cobalt tube operated at 38 kV and 38 mA. Samples were scanned from 5 to 90 degrees at a speed of 2 degrees 2-theta per minute, with a step size of 0.02 degrees. The obtained data was interpreted using Jade 9.1 and the 2011 ICDD and 2011 ICSD databases.

3.2.5 X-Ray Photoelectron Spectroscopy

X-Ray Photoelectron Spectroscopy **(**XPS) was used to look at the bonding as well as the qualitative composition of the surface. XPS was performed at the University of Alberta in the Alberta Center for Surface Engineering and Science (ACSES) by a trained technician. An AXIS 165 spectrometer with a monochromatic Al Kα source (1486.6 eV) was used for the analysis. The instrument base pressure was less than $5x10^{-8}$ Pa. Analysis was completed on a 400 x 700 μm area with a pass energy of 160 eV or 20 eV for high resolution. The resolution for the instrument is 0.55 eV for Ag 3d and 0.70 eV for Au 4f. The spectra were analyzed using CasaXPS software. The instrument was calibrated by setting the Fe(III)-O peak to 711 eV.[48]

3.2.6 CHNS Elemental Analysis

An Elementar Vario Microcube elemental analyzer (CHNS) was used to measure the carbon, hydrogen, nitrogen and sulfur content within the produced liquid and coke samples following bitumen cracking. The CHNS was operated based on a trained technician’s advice ensuring that all of the recommend temperatures, pressures and flows were acceptable. Furthermore, five blank samples were initially run to remove any contaminants existing in the equipment. This was followed by two run-in and three standard samples, all containing approximately 2 mg of sulfanilic acid. The pro analysis sulfanilic acid was obtained from Merck and used as the standard. For each analysis, triplicates were completed with 2-3 mg of sample being loaded into 4x4x11 mm tin boats. Data was interpreted using the Vario software.

3.2.7 Surface Area Analysis

Five-point Brunauer-Emmett-Teller (BET) surface area analysis of α-Fe_2O_3 and FeS were completed using a Micrometrics ASAP 2020 analyzer. Sufficient sample was accurately weighed and loaded into a glass sample tube such that the total surface area was 1-10 m^2. The sample was then degassed at 250 °C for two hours prior to analysis. Following degassing the sample was re-weighed to obtain an accurate weight without any absorbed gases. The sample was attached to the analysis port and cooled to 77 K to allow the nitrogen adsorbate to condense on the sample using a dewar of liquid nitrogen. The 5-Point BET analysis was started and analyzed using ASAP 2020 analysis program.

Chapter 4: Results and Discussion

4.1 Effect of Steam and α-Fe_2O_3 on the Liquid Phase Cracking of Hexadecane

The primary upgrading of bitumen is often completed by carbon rejection technologies, which, redistribute the hydrogen to produce a fraction with a higher hydrogen content and a fraction (coke) with a lower hydrogen content.[18] Unfortunately, due to the high heteroatom content, coke produced during bitumen upgrading is of low value and is thus stockpiled.[2] It would therefore be useful to reduce the coke yield in order to increase the overall feed efficiency. Fumoto *et al*. showed that the combination of steam and α-Fe_2O_3 resulted in a reduction in the total coke yield during the cracking of atmospheric residue.[8] To gain a better understanding of this mechanism, the model compound n-hexadecane was used to evaluate the catalytic cracking properties of α-Fe_2O_3 in the presence of steam. Figure 4-1 presents the conversion of hexadecane after cracking in the liquid phase for 45 minutes at 420 °C in the presence and absence of both α-Fe_2O_3 and steam.

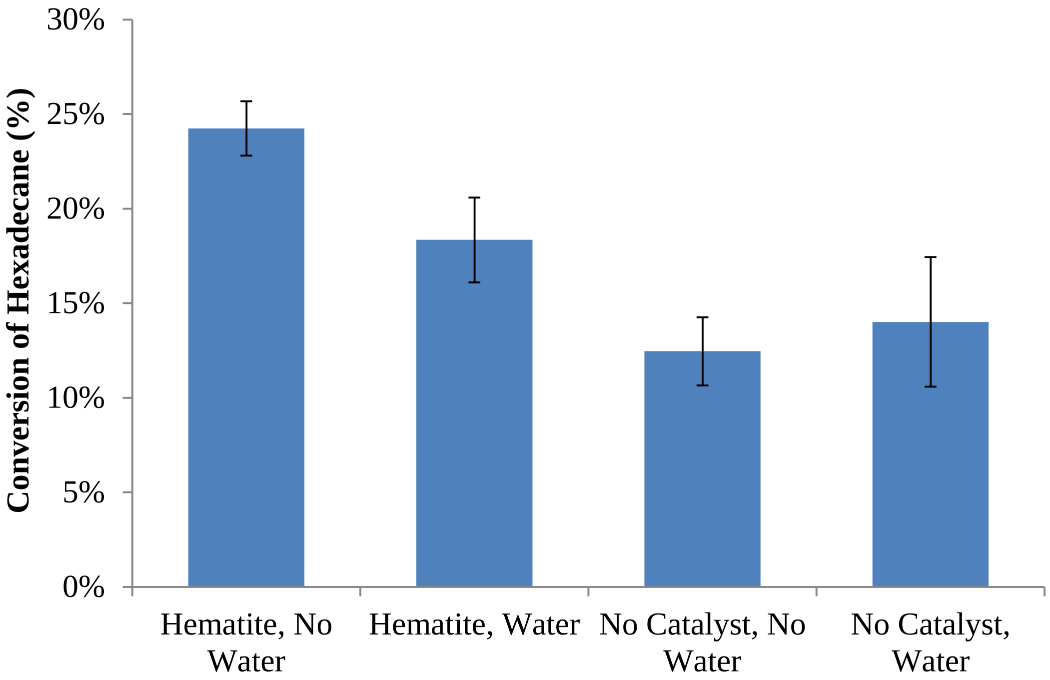

Figure 4-1. Conversion of hexadecane after cracking at 420°C for 45 minutes with 95% confidence interval

Under an inert nitrogen atmosphere and without the addition of α-Fe_2O_3, the conversion of n-hexadecane was determined to be 12.5%. To validate the method, the predicted conversion was calculated for a residence time of 45 minutes using the data provided by Ford.[33] In his paper, Ford, calculated the first order rate constants at 330 °C, 350 °C and 370 °C.[33] Unfortunately, these temperatures are below that used in this study and thus some extrapolation must be done, introducing a source of error. By linearizing the Arrhenius equation (4-1), the pre-exponential factor and the activation energy was calculated. As was shown earlier, at a set point of 420 °C, the true temperature of the sand bath is 415 °C. By using the true temperature of 415 °C, the first order rate constant was calculated to be 0.1719 hour^{-1}. The calculated rate constant was then used to solve the design equation for a batch reactor (4-2) with a residence time of 45 minutes and produced a theoretical conversion of 12.1%. A conversion of 12.1% is within error of this experimental method and therefore validates the results obtained. This means that the thermal cracking of hexadecane propagated via the same mechanism as proposed by Ford[33] and that thermal cracking should not be ignored when studying the role of α-Fe_2O_3.

$$k = A\exp\left(\frac{-Ea}{RT}\right) \tag{4-1}$$

$$\frac{dC_A}{dt} = -kC_A \tag{4-2}$$

Two-way analysis of variance was used to interpret the conversion data and to determine the individual effect of α-Fe_2O_3 and steam, as well as the interaction between the two. Individually, it can be said that α-Fe_2O_3 increases the conversion of hexadecane, while the addition of steam alone does not cause a significant change in the conversion. On the other hand, when we explore the interaction of α-Fe_2O_3 and steam, it is found that the interaction causes a statistically significant change in the conversion.

Liquid phase thermal cracking of hexadecane proceeds via a free-radical chain reaction and at low conversions results in the equimolar production of alkanes and alkenes.[33, 34, 36] Figure 4-2 presents the alkane to alkene ratio as a function of carbon number. Methane, as well as all n-alkanes and 1-alkenes from C_2-C_{15} were formed during this reaction. In addition, internal alkenes were also observed using GC and GC-MS for all hydrocarbons from C_4 to C_{14}. Given that water has been shown to not impact conversion, both cases containing no α-Fe_2O_3 resulted in an alkane to alkene ratio consistent with that of liquid phase thermal cracking. On the other hand, when α-Fe_2O_3 is added to the reaction medium, the alkane to alkene ratio increases to approximately 2. This is consistent with the mechanism of catalytic cracking in which the alkane to alkene ratio is greater than 1.[74] It is also observed that the addition of steam causes a decrease in the alkane to alkene ratio indicating that the steam is interacting with the active sites. Finally, in the presence of α-Fe_2O_3, internal alkenes are produced but their production is inhibited by the presence of water. The increase in the conversion, alkane to alkene ratio and internal alkenes are all indicators of an acid catalyzed process.

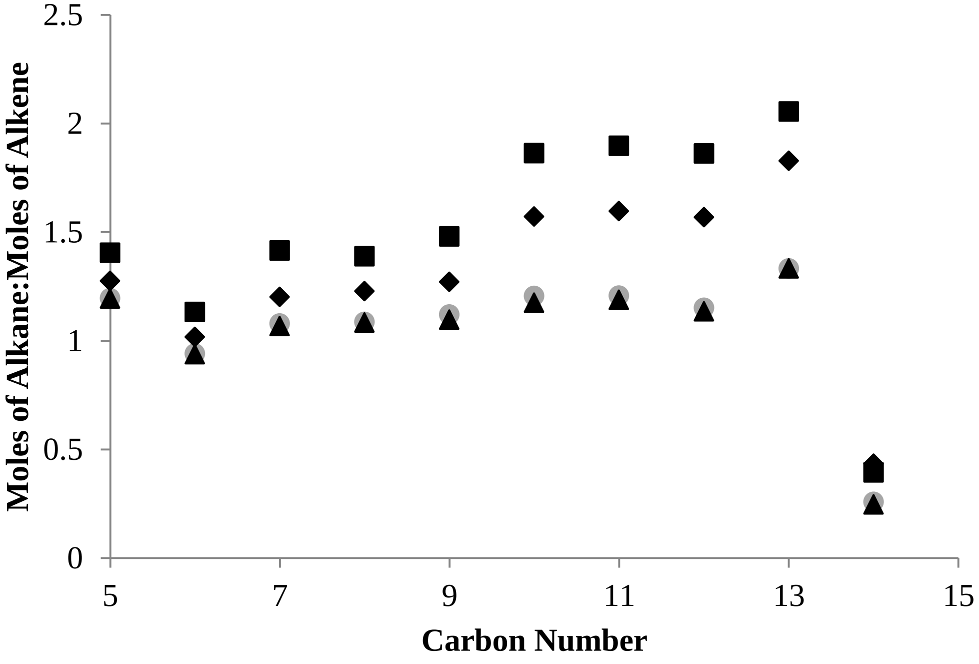

Figure 4-2. Alkane-to-Alkene ratio for the produced liquid product from the cracking of hexadecane at 420 °C for 45 minutes (■-Hematite, No Water, ●-No Catalyst, No Water, ▲-No Catalyst, Water, ♦ - Hematite, Water)

It should be pointed out that, as expected, a significant decrease in the alkane to alkene ratio is observed at a carbon number of 14. Considering the mechanism for the thermal cracking of an n-alkane, it is required that in order to produce n-tetradecane through β-scission a primary hexadecyl radical must be present. Wu *et al*.[34] points out that a secondary radical is 16.8 kJ/mol more stable than a primary radical and thus the preferred orientation, while the activation energy for the cracking of primary radical is 125.6 kJ/mol.[36] Furthermore, the activation energy for isomerisation via internal hydrogen transfer is 48.9-78.3 kJ/mol,[36] while the activation energy for the abstraction of hydrogen by a primary radical has previously been reported to be 48.9-58.6 kJ/mol.[36] It is therefore more likely that the primary radical will either stabilize itself via isomerisation or hydrogen abstraction rather than cracking and thus reducing the yield on n-tetradecane. On the other hand, a hexadecyl radical with the radical located on the fourth carbon can crack to produce tetradecene and ethane more easily, resulting in the low alkane to alkene ratio. The concentration of carbon 15 compounds was too low to measure. To produce a carbon 15 molecule a hexadecyl radical with the radical located on the third carbon is required to crack and produce a methyl radical. The methyl radical is significantly less stable than even the ethyl radical, which can be stabilized by hyperconjugation, and therefore has an activation energy of at least 8.4 kJ/mol higher than would be required to crack a similar hexadecyl radical to produce 1-butene and a dodecyl radical.[34] Therefore, the preferred route for cracking of a hexadecyl radical, with the radical located third carbon, results in the production of dodecane and 1-butene.

Catalytic cracking occurs on the surface of the catalyst through either Bronsted (proton donating) or Lewis (electron pair accepting) acid sites. It is known that, although not present in the bulk, the surface of α-Fe_2O_3 contains hydroxyl groups bound in either a singly, doubly, triply or geminal configuration.[49] Using 2,6-dimethyl pyridine and pyridine Ferretto *et al*. was able to show that synthesized hematite contained hydroxyl groups capable of donating protons.[48] This is in contrast to other studies that have noticed little to no protonation of pyridine indicating that any Bronsted acidity is likely very weak.[54] To verify the existence of hydroxyl groups, XPS was performed on the catalyst, prior to the reaction as is shown in Figure 4-3. The O 1s XPS spectra provides the fitted curve for the experimental data, as well as the three distinct individual peaks for the oxygen in different electronic environments. The raw XPS data can be found in Appendix A. The peak at 529.1 eV is assigned as O^{2-} or the oxygen within the iron oxide lattice, which is slightly lower than the literature value of ≈530.0 eV.[52, 75, 76] The second major peak at 530.9 eV is assigned to –OH, but is again slightly lower that the literature value of 531.6 eV.[52, 76] Finally, the minor peak can be at 533.3 eV is oxygen contained within water.[52, 76] The bond energies reported in literature for the oxide and hydroxyl oxygen, are different from those reported in this study, due to how the binding energies were aligned. In the study by Yamamoto *et al*.[52] the oxide peak was fixed at 530.0 eV, whereas the oxygen peak in this study was shifted based on the iron peaks. If a similar approach had been used, the hydroxyl peak would move to approximately 531.8 eV and line up well with previous studies.

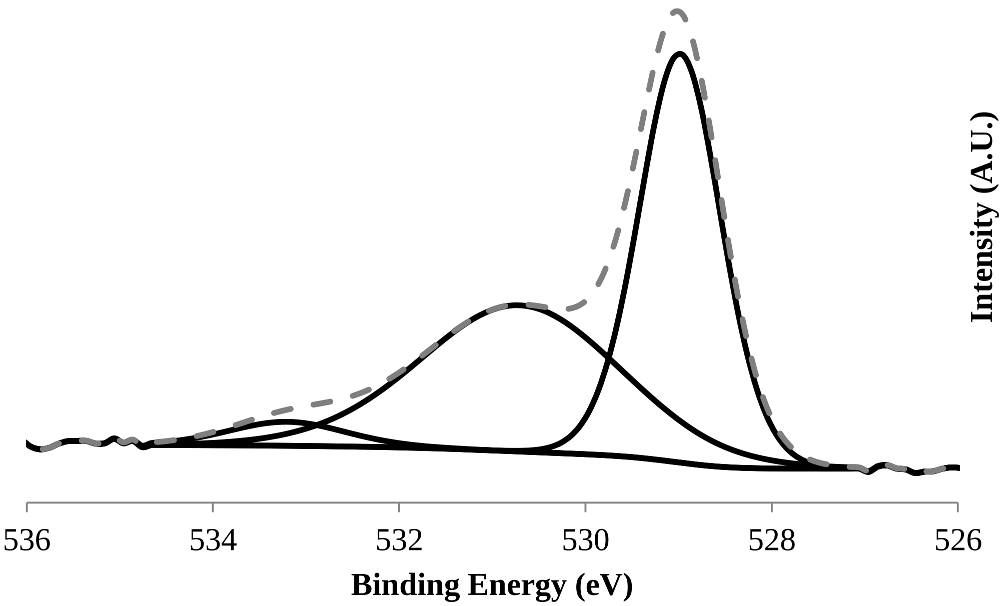

Figure 4-3. O 1s XPS spectra of α- Fe_2O_3 prior to reaction and without cleaning. Raw data(located in Appendix A) is not shown for clarity, but the overall curve fitted to the raw data is displayed (dotted line). Individual curves are displayed for the three types of oxygen (solid lines). Oxygen contained in free water at 533.3 eV, hydroxyl surface groups at 530.9 eV and structural O^{2-} at 529.1 eV.

As shown, Bronsted acid sites are present and capable of catalyzing protolytic cracking. Lewis acid sites are present on α-Fe_2O_3 as shown by adsorption of pyridine on the surface.[48] Thus, it is expected that both Bronsted and Lewis sites are present during the reaction. Regardless of how catalytic cracking is initiated, the formation of a carbenium ion[45] can occur and propagate the reaction. Upon the formation of the carbenium ion, a number of pathways including β-Scission, disproportionation and oligomerization may proceed. Based on the increase in conversion, catalytic β-scission of hexadecane must be occurring, resulting in the production of an alkene and an alkane. However, this alone cannot explain the increase in the alkane to alkene ratio which, based on catalytic β-scission, should be 1.[45] Similar to thermal cracking, the probability of a bimolecular reaction occurring increases within the liquid phase. The increase in bimolecular reactions would explain the increase in the alkane to alkene ratio as well as the absence of branched alkanes smaller than the parent hexadecane molecule. Disproportion is the reaction between a carbenium ion and an alkane causing the formation of a larger carbocation,[46] which can crack, resulting in the formation of an alkane and a smaller carbocation. The problem with this mechanism is that it would be expected that branched alkanes would be observed because, as Sie *et al*.[77] points out, tertiary carbocations are significantly more stable than primary carbocations. Thus, the carbocation would be expected to rearrange to have the cation on one of the secondary carbons leading to, upon addition, a branched carbocation which when cracked would produce a branched alkane. No non-linear alkanes were observed, leading to the conclusion that disproportiation was at most a minor reaction pathway. Bassir and Wojciechowski[78] observed similar results with n-hexane where bimolecular reactions became unimportant likely due to the absence of an tertiary carbons. Therefore the increase in the alkane to alkene ratio must be due to the reaction of a carbocation with an alkene resulting in a formation of a larger carbocation, which can crack resulting in an alkene or abstract a hydride ion from a hexadecane molecule and desorb[47] to produce a branched alkane larger than C_{16}. Indication of this occurring can be seen by the fact that the alkane to alkene ratio is increasing, while the quantity of addition products is increasing as shown in Figure 4-4.

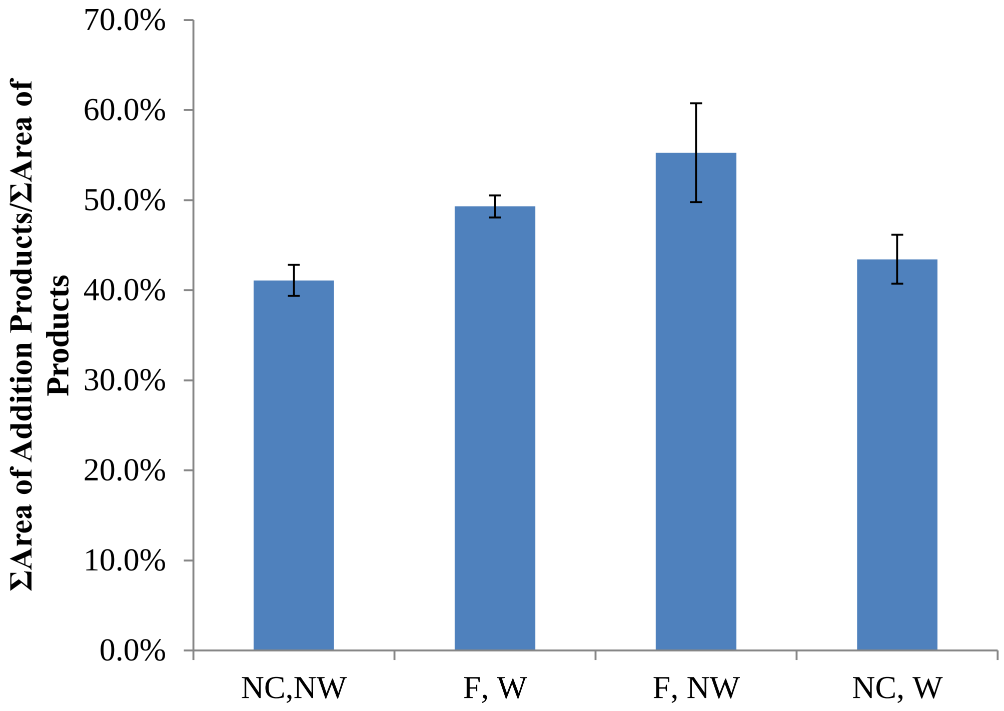

Figure 4-4. Percentage of total products with a carbon number greater than 16. Calculated by take the sum of the area greater than C_{16}/sum of the total products. Error bars presented correspond to a 95% confidence interval. (NC=No Catalyst, NW=No Water, F=α-Fe_2O_3, W=Water)

To explain the decrease in conversion and the alkane to alkene ratio when water is added, the role of water must be examined. Previous work has argued that the inclusion of water can transform Lewis acid sites into Bronsted acids[79] on heterogeneous catalysts, which would be expected to produce an increase in the conversion, addition products and the alkane to alkene ratio, none of which occurred. No studies on the interaction between α-Fe_2O_3 and water have been found using the temperatures or pressures utilized in this study. With that in mind, previous work has shown that under ambient conditions water can dissociate resulting in hydroxylation of the surface[52] and the expectation that the surface of the catalyst is saturated with hydroxyl groups. Since no pre-treatment was completed, the number total number of hydroxyl groups will not increase when water is added. Numerous studies have shown that once the surface is hydroxylated, a physisorbed layer of water is formed via hydrogen bonding,[80-82] with McCafferty and Zettlemoyer[81] demonstrating that water can be stabilized by two hydroxyl groups. It is therefore hypothesized that the water is interacting with the surface, via hydrogen bonding and molecular adsorption, as shown in Figure 4-5. The second proposed mechanism of inhibition is by molecular adsorption on the Lewis acid sites. As the α-Fe_2O_3 is heated the hydroxyl groups may also condense resulting in the formation of a Lewis acid site.[54] These or any Lewis sites are then capable of interacting with the lone pair of electrons on the oxygen and undergo either molecular adsorption or dissociation.[53] If molecular adsorption occurs, hydrocarbons will be inhibited from interacting with the site. Similar results have been observed using benzene where water prevents the interaction between the π-bonds and the acid site.[56] Finally, it has also been calculated that it is possible for water to undergo molecular adsorption on a ferryl (F=O) termination.[53] Although the dissociation has been deemed unimportant for this reaction, its occurrence cannot be rejected. However, it is expected that if dissociation does occur it will either be removed immediately without reacting with a hydrocarbon or be blocked from reacting by the formation of physisorbed water layer.

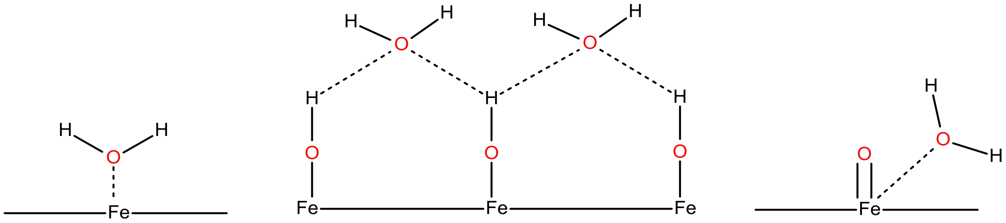

Figure 4-5. Potential interaction of water with the iron oxide surface[53, 81, 82]

While it appears that the increased conversion and alkane to alkene ratio is due to catalytic cracking, it may also be due to the complete oxidation by α-Fe_2O_3. As Table 4-1 shows, the addition of α-Fe_2O_3 results in a higher concentration of carbon dioxide, indicating that a fraction of the hydrocarbon medium has been completely oxidized. It also appears that when water and α-Fe_2O_3 are present the concentration of CO_2 is higher than when water is absent. To produce CO_2, α-Fe_2O_3 must be reduced to Fe_3O_4 and FeO, however, Fe_3O_4 cannot be oxidized back to Fe_2O_3 with steam.[63] Therefore, the total mass of carbon dioxide cannot be increased, implying that less gas is actually produced and agreeing with the lower overall conversion.

Table 4-1. Molar gas composition following the cracking of hexadecane at 420 °C for 45 minutes(NC=No Catalyst, Fe= α-Fe_2O_3, W= Water, NW = No Water)

	NC, NW (mol%)	**NC, W (mol%)**	**Fe, NW (mol%)**	**Fe, W (mol%)**
CH_4	8.66 ± 0.75	8.74 ± 1.18	9.69 ± 0.18	8.70 ± 1.05
CO_2	0.42 ± 0.73	0.69 ± 0.25	8.65 ± 1.01	12.82 ± 2.82
C_2H_4	5.07 ± 0.13	5.22 ± 0.39	3.63 ± 0.11	4.12 ± 0.48
C_2H_6	26.90 ± 1.63	25.99 ± 1.35	27.75 ± 0.79	24.12 ± 2.47
C_3H_6	15.30 ± 0.33	15.00 ± 0.21	12.96 ± 0.62	12.30 ± 0.79
C_3H_8	16.42 ± 0.61	15.61 ± 0.20	16.64 ± 0.39	13.82 ± 0.94
1-C_4H_8	5.34 ± 0.50	5.38 ± 0.40	3.41 ± 0.08	4.15 ± 0.30
C_4H_{10}	6.69 ± 0.69	6.41 ± 0.43	6.70 ± 0.09	6.02 ± 0.45
2-C_4H_8	0.23 ± 0.08	0.24 ± 0.07	0.67 ± 0.06	0.40 ± 0.07
C_5+	14.62 ± 4.78	15.27 ± 2.37	9.89 ± 1.50	13.55 ± 3.29
CO	0.34 ± 0.59	1.46 ± 0.25	0 ± 0	0 ± 0

No studies have been found that examine the rate of oxidation of alkanes and alkenes by α-Fe_2O_3 in the liquid phase or pertaining to the oxidation of linear alkanes and alkenes in the absence of oxygen. However, previous literature has indicated that α-Fe_2O_3 in the presence of oxygen oxidizes gaseous propene faster than propane,[83] while a separate study using Pt/Al_2O_3 showed that the reactivity of n-alkanes increases with chain length.[84] In addition, through the use of Pt/Al_2O_3, n-alkenes were found to be more reactive then the corresponding alkanes and their reactivity did not depend on their chain length.[83] Based on these trends and given the fact that α-Fe_2O_3 is expected follow similar trends to other metal oxides[83], it is expected that hexadecane would be more easily oxidized than any of the smaller alkanes. This would cause more hexadecane to be converted into carbon dioxide and ultimately result in an increase in the hexadecane conversion. As Figure 4-1 shows, there is approximately a 12% increase in conversion when only α-Fe_2O_3 is present compared to the case of thermal cracking. If we consider the fact that α-Fe_2O_3 is reduced to Fe_3O_4 in the absence of water, as shown in Figure 4-6, and assume complete combustion (equation 4-6), it can be found that the increase in conversion is not solely due to catalytic oxidation. To determine the effect of oxidation, a balanced equation was produced for the complete oxidation of hexadecane. By using the same conditions as used in these reactions (*i.e.* 3 g hexadecane), it was calculated that the stoichiometric reduction of hexadecane would require 37.3 g of α-Fe_2O_3. Considering that only 0.3 g of α-Fe_2O_3 was actually added, it appears that oxidation is, at most, a minor pathway. Furthermore, this calculation also assumes that only hexadecane would be oxidized, which is also incorrect given that alkenes are known to be more reactive than alkanes. By comparison, if the α-Fe_2O_3 were reduced solely due to its reaction with hexadecane, this would only account for a change in the conversion of approximately 0.1%. This insignificant conversion leads to the conclusion that, that the increased conversion is not due to the catalytic oxidation of hexadecane.

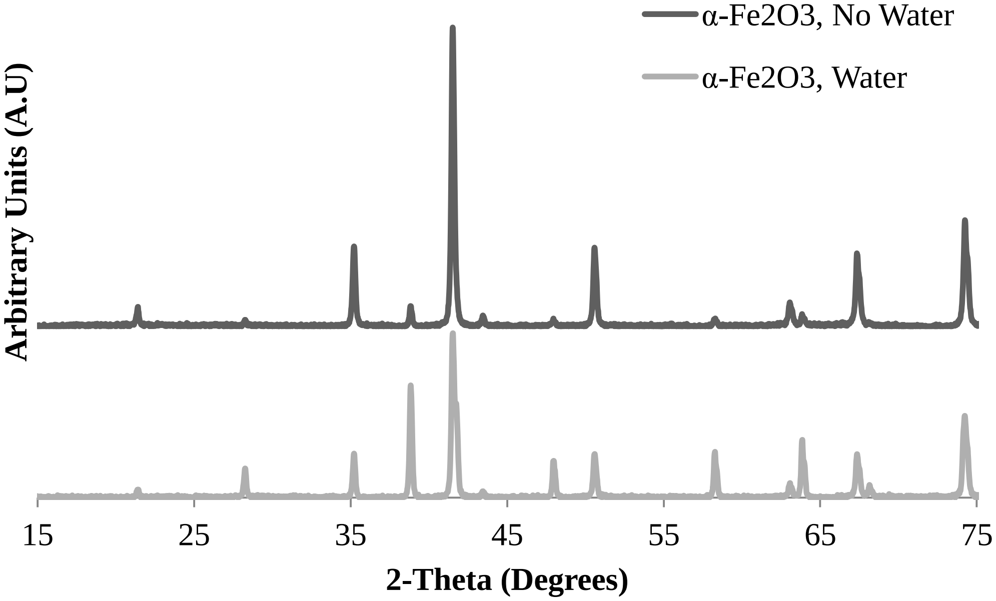

Figure 4-6. X-Ray diffraction pattern for the iron oxide catalyst following cracking of hexadecane at 420 °C for 45 minutes

The second characteristic that needs to be considered is the alkane to alkene ratio. As previously mentioned, it is known that, alkenes are more reactive than alkanes,[83] leading to the hypothesis that an increase in the alkane to alkene ratio may be simply due to the alkenes being oxidized to carbon dioxide. If both assumptions that the reactivity of the alkenes is nearly constant regardless of chain length and that the alkane reactivity increases with chain length holds true, then it is expected that the alkane to alkene ratio would decrease with increasing chain length. This is the opposite of what is seen in Figure 4-2, where the alkane to alkene ratio actually increases with carbon number. Furthermore, if either the conversion or the alkane to alkene ratio was the result of oxidation it would be necessary for the total gas yield to increase from the cases without α-Fe_2O_3. This was not observed and furthers the idea that oxidation plays a minimal role in the reaction network.

These findings lead to the conclusion that α-Fe_2O_3 cracks hexadecane via its active acid sites resulting in an increase in the conversion, alkane to alkene ratio and addition products. The reduction to Fe_3O_4 and subsequent oxidation of hydrocarbons only plays a minor role in the reaction pathway, while the addition of water causes a reduction in the overall conversion and other indicators of catalytic cracking due to blocking of active sites.

4.2 Effect of sulfur on the hexadecane, α-Fe_2O_3 and water system

During the cracking of bitumen, hydrogen sulfide is formed through the decomposition of alkyl sulfides. Iron oxides, including α-Fe_2O_3 are known to react with hydrogen sulfide to produce iron sulfides.[12, 13] It is therefore important to investigate the impact of sulfur, specifically sulfides, on the decomposition of hexadecane in the presence of α-Fe_2O_3 and steam. To test the impact of sulfur, 3300 ppm of sulfur in the form of dimethyl disulfide was added to the reaction medium. Dimethyl disulfide is known to decompose to produce hydrogen sulfide under similar reaction conditions,[37, 70, 71] through a chain reaction involving the abstraction of hydrogen from other hydrocarbons. Upon completion of the reaction, the catalyst, liquid and gas were separated and analyzed. To ensure that the presence of water was not inhibiting the decomposition of the dimethyl disulfide, the sulfur concentration of the liquid product was measured. In the presence of steam the liquid contained 384.2 ppm of sulfur with a relative standard deviation of 8.91% compared to the case without steam, which contained 355.7 ppm with a relative standard deviation of 9.32%. Since hydrogen sulfide can dissolve in the liquid hydrocarbon and given the relatively small difference between the samples, it can be concluded that steam is not preventing dimethyl disulfide from decomposing.

The concentration of the produced gas was measured using GC. Figure 4-7 presents a fraction of the chromatogram for the cracking of hexadecane and dimethyl disulfide with α-Fe_2O_3 in the presence and absence of water. Also shown for comparison is a chromatogram for the cracking of hexadecane with α-Fe_2O_3 but in the absence of water and dimethyl disulfide. Although both an FID and TCD was used for quantification, the FID signal is omitted as the response factor of the hydrogen sulfide was too low causing the intensity of the hydrocarbon peaks to dominate the chromatogram. Therefore, to increase clarity only the chromatograms obtained with a TCD are presented. It should be noted that the peak intensities for runs containing no water cannot be directly compared to the runs containing water. In order to account for the partial pressure of steam, an increased initial nitrogen pressure was required which lowers the gas-phase concentration of each component and results in reduced peak intensities.

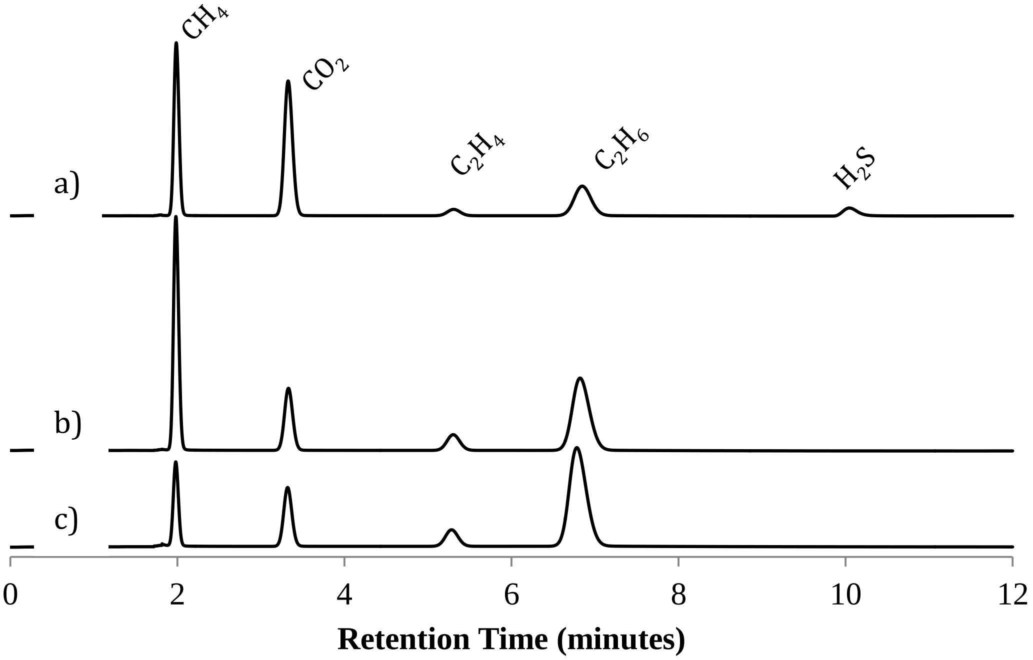

Figure 4-7 Chromatogram for the cracking of hexadecane with a)dimethyl disulfide, α-Fe_2O_3 and water (W), b) dimethyl disulfide (DMDS) and α-Fe_2O_3 (Fe) and c) α-Fe_2O_3 with no water or dimethyl disulfide

The first noticeable trait is the significant increase in the amount of methane produced when hexadecane is cracked with dimethyl disulfide. In the presence of α-Fe_2O_3, but without water or dimethyl disulfide, the height of the methane peak is approximately equivalent to the ethane peak. On the other hand, when dimethyl disulfide is added to the reaction medium the ratio of peak heights for the methane peak to the ethane peak is substantially higher, indicating a higher concentration of methane. The increased methane content is a result of the decomposition of dimethyl disulfide, resulting in the formation of 2 moles of methane per mole of dimethyl disulfide. The increased concentration of methane is also an indicator of the cleavage of the sulfide bonds. It should also be noted that no peak for dimethyl disulfide was ever detected. In an attempt to identify a dimethyl disulfide peak, the 3300 ppm solution was loaded into a reactor and pressurized with nitrogen. The pressurized reactor was then agitated, but not heated, to bring the gas and liquid to equilibrium. By bringing the phases to equilibrium, a gas phase with the maximum possible concentration of dimethyl disulfide was created and injected into the GC. Since no dimethyl disulfide was detected, the lower sulfur concentration of the liquid and the hydrogen sulfide formation must be used as indicators that the dimethyl disulfide has undergone near complete decomposition.

The second characteristic of interest is the hydrogen sulfide peak at a retention time of 10 minutes, confirming that dimethyl disulfide is producing hydrogen sulfide as one of its decomposition products. Furthermore, as can be noted by the decreased hydrogen sulfide peak intensity, when the water is removed a reduction in the concentration of hydrogen sulfide is observed. The decreased concentration is likely due to the adsorption of the hydrogen sulfide by the iron oxide. Hydrogen sulfide is capable of reacting with Fe_2O_3 and Fe_3O_4 to produce iron sulfide via reactions 4-3 and 4-4.[12, 13] Iron sulfide can also be produced by the reactions described in equations 4-5,[65] where hydrogen sulfide reacts directly with α- Fe_2O_3 to produce Fe_2S_3 (4-5a), which is thermodynamically unstable and reduces immediately to FeS_2 and Fe_3S_4 (4-5b).

$$Fe_2O_3 + H_2 + 2H_2S \longleftrightarrow 2FeS + 3H_2O \tag{4-3}$$

$$Fe_3O_4 + H_2 + 3H_2S \longleftrightarrow 3FeS + 4H_2O \tag{4-4}$$

$$Fe_2O_3 + 3H_2S \longrightarrow Fe_2S_3 + 3H_2O \tag{4-5a}$$

$$2Fe_2S_3 \longrightarrow FeS_2 + Fe_3S_4 \qquad \text{4-5b}$$

For 4-3 and 4-4 to proceed, hydrogen must be available to the reaction network. Although not initially present, hydrogen is formed through a number of side reactions. The oxidation of hexadecane produced a significant amount of carbon dioxide through oxidation with α-Fe_2O_3. As shown by Ryden *et al.*, the oxidation of methane with α-Fe_2O_3 can produce carbon dioxide and water (4-6) or carbon monoxide and water due to incomplete combustion (4-7).[62]

$$CH_4 + 12Fe_2O_3 \longrightarrow 8Fe_3O_4 + CO_2 + 2H_2O \qquad \text{4-6}$$

$$9Fe_2O_3 + CH_4 \longrightarrow 6Fe_3O_4 + CO + 2H_2O \qquad \text{4-7}$$

As shown in Table 4-1, in the presence of α-Fe_2O_3, no carbon monoxide is detected. This lack of carbon monoxide can be explained by the reaction proceeding only by complete oxidation or by the fact that the iron oxide may act as a catalyst for the water gas shift reaction (4-8)[85] and lead to the formation of hydrogen and carbon dioxide. Although not leading to hydrogen, it is also possible that the carbon monoxide is absent because it has been oxidized by Fe_2O_3 to produce CO_2.[62]

$$CO + H_2O \longleftrightarrow H_2 + CO_2 \qquad \text{4-8}$$

Hydrogen can also be produced during a side reaction from the cracking of hexadecane. Gas-phase reactions have shown that β-hydrogen may be cleaved rather than the β-carbon (4-9) resulting in a hydrogen radical, free to propagate the reaction via hydrogen abstraction to produce H_2 (4-10).[30] Cleavage of the C-H bond, however, is expected to be a minor reaction pathway in comparison to C-C cleavage based on the bond dissociation energies.[37] Although possible, reactions

4-6 to 4-10 are all minor reaction pathways and therefore, the total hydrogen content will be quite low and the formation of iron sulfide is predicted to predominantly follow reactions (4-5a) and (4-5b). Unfortunately, helium was used as the carrier gas during the GC analysis of the produced gas and therefore the formation of hydrogen could not be detected by the TCD.

$$R-H\overset{\bullet}{C}-C\,H_3 \longleftrightarrow R-HC=CH_2+\overset{\bullet}{H} \tag{4-9}$$

$$\overset{\bullet}{H}+C_{16}H_{34} \longleftrightarrow \overset{\bullet}{C}_{16}\,H_{33}+H_2 \tag{4-10}$$

Based on the known reactions of iron oxides with hydrogen sulfide and the disappearance of hydrogen sulfide from the produced gases in the absence of water, it is expected that iron sulfide is being produced. As previously mentioned in the presence of water the cracking of hexadecane by α-Fe_2O_3 is inhibited due to the steam interacting with the surface of the catalyst and inhibiting the surface reactions. Therefore, it can also be said that the increased hydrogen sulfide gas concentration in the presence of water is also due to the inhibiting nature of the steam on the iron oxide surface, preventing the formation of iron sulfide. To further test the theory that steam was preventing the hydrogen sulfide-iron oxide reaction from occurring, XPS was used to characterize the surface of the iron oxide particles after the reaction. XPS was used to determine not only the qualitative elemental composition, but also to understand the bonding. Figure 4-8 shows the binding energies corresponding to the Fe 2p region in both the absence and presence of steam. To increase clarity, only the raw data, background and the overall fitted curve are included, while the individual curves corresponding to Fe(II)-O, Fe(III)-O and Fe-S have been omitted.

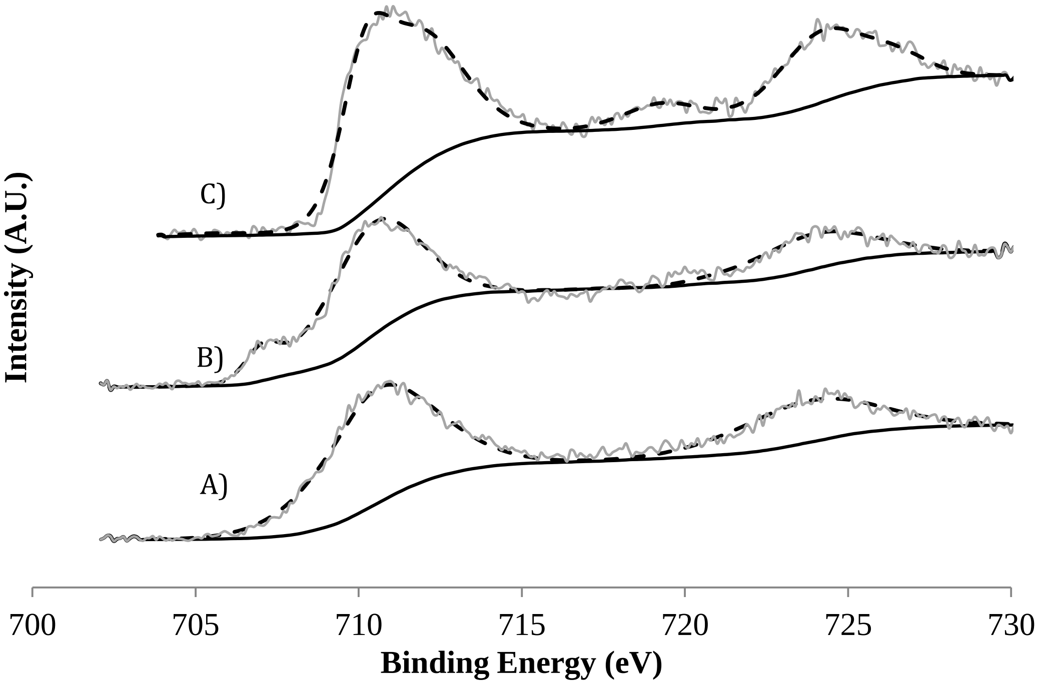

Figure 4-8. Fe 2p spectrum of the iron oxide catalyst following the cracking of hexadecane and dimethyl disulfide in the a)presence of steam and in the b) absence of steam c) fresh α-Fe_2O_3.The dotted line (----) represents the fitted curve for all the data, while the solid gray line is the raw data. The individually fitted curves are presented in Appendix A. Peaks at 711 eV is characterized as Fe(III)-O, while peak at 706 eV is characterized as Fe-S.

As can be seen, all cases show peaks with binding energies of approximately 711 and 724 eV, but an extra peak appears at 706 eV when hexadecane and dimethyl disulfide are cracked with α-Fe_2O_3, but without steam. Previous literature has classified the peaks at 725 eV to be satellite peaks, while those at approximately 711 eV to Fe(III)-O peaks.[48, 86] On the other hand, based on previous literature, the extra peak at 706 eV could be either Fe(II)-S[87] or simply metallic iron.[86] Given that this peak occurs in the absence of steam, there are two possible explanations to consider. First, the peak may be from the reaction of iron oxide with hydrogen sulfide to produce iron sulfide. The second possibility is that this peak may be the metallic iron due to either the reduction of Fe_3O_4 to Fe or to the presence of metallic iron present within the initial catalyst which, when heated in the presence of steam is oxidized into iron oxide causing the elimination of the peak at 706 eV. To determine the true nature of this peak the surface of the non-reacted sample of α-Fe_2O_3 was analyzed and is also seen in Figure 4-8. The lack of a peak in the non-reacted sample confirms that no metallic iron is present and that the peak at 706 eV is either Fe from the reduction of Fe_3O_4 or Fe-S.

To determine if the unknown peak is Fe-S, the S 2p region was analyzed and corroborates the idea that α-Fe_2O_3 is reacting to form an iron sulfide material. Figure 4-9, displays the S 2p region of the reacted solids and shows an increased amount of sulfur on the catalyst surface in the absence of water. Displayed is the overall fitted curve (dashed line) as well as the curves fitted for each individual peak. These spectra can be split into two sections at 161 eV and 166 eV, corresponding to sulfate and sulfide species, respectively.[87, 88] When comparing the two spectra, the intensities of the peaks are significantly different indicating that more sulfur is present when no water is added. This confirms that under these reaction conditions the α-Fe_2O_3 can react with H_2S. Further interpretation of this region also shows that the majority of sulfur is in the sulfide state. The four peaks in the sulfide region correspond well to literature and are identified as FeS (160 eV), polysulfides (161.5 and 162.9 eV) and elemental sulfur (164.1 eV).[87, 89] Davydov *et al*. attributes the formation of elemental sulfur to the coupling of the reduction of Fe(III) to Fe(II) with S^{2-} to S_x.[65] Given that the reactor was purged of all oxygen, the formation of iron sulfates is expected to be due to the oxidation of the produced iron sulfides upon opening of the reactor system.

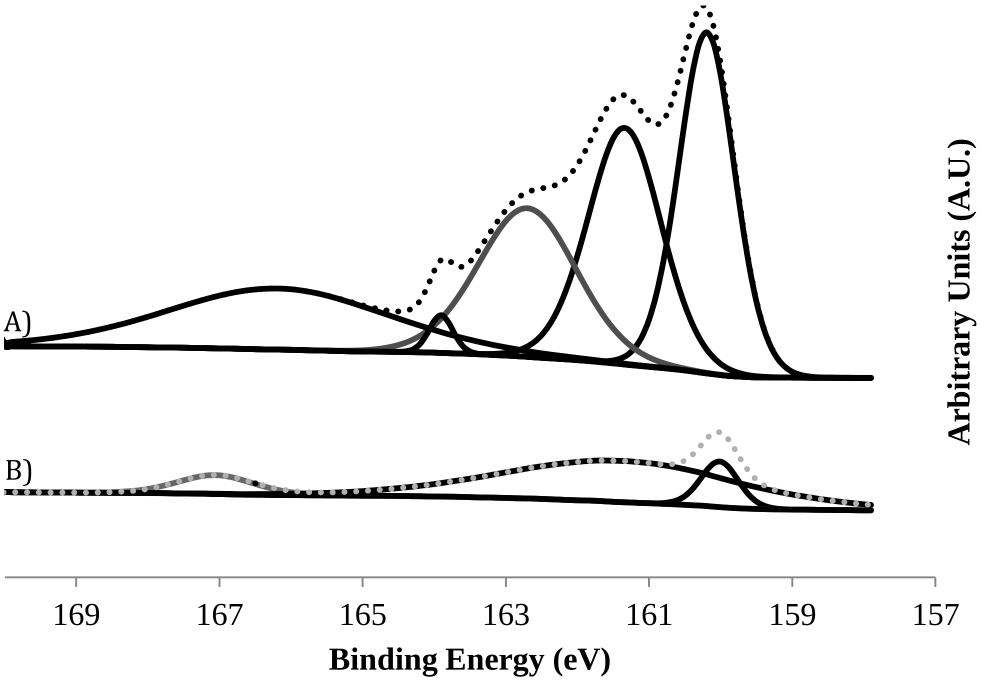

Figure 4-9. S 2p spectrum of the iron oxide catalyst following the cracking of hexadecane and dimethyl disulfide in the a)absence of steam and in the b)presence of steam. The dotted line (•••) represents the curve fitted to the raw data, while the solid lines are the individually fitted curves representing various electronic environments. The Raw data is presented in Appendix A. The peaks can be identified as FeS (160 eV), Polysulfides (161.5 and 162.9 eV), elemental sulfur (164.1 eV) and sulfates (166 eV).

It has been shown that when steam is present the amount of sulfur within the catalyst is reduced, likely due to the steam simply inhibiting the reaction by competing for similar sites. Davydov *et al.*[65] produced a mechanism for the oxidation of H_2S by α-Fe_2O_3. In this mechanism, the lone pair of electrons on the sulfur interacts with the unsaturated iron center while the hydrogen within the H_2S hydrogen bonds to the lattice oxygen. Given the structure of water, it is expected that a similar coordination occurs resulting in the blocking of surface sites for H_2S

to adsorb on. It is also possible, however, that the steam is oxidizing the produced FeS to an iron oxide species. To test the oxidation theory as well as the impact of iron sulfide on the cracking of the hexadecane, FeS was used as a catalyst in place of α-Fe_2O_3. As Table 4-2 indicates, the inclusion of steam in the reaction medium results in the formation of hydrogen sulfide. Since FeS is the only source of sulfur, it is necessary that the formation of hydrogen sulfide be due to steam oxidation. It should also be noted that the amount of carbon dioxide and carbon monoxide formed is within error for the cracking cases involving hexadecane with and without water as shown in Table 4-1. This indicates that no carbon oxides were formed from the catalyst and all of the carbon oxides are due to reactions with the reactor walls.

Table 4-2. Molar gas composition from the cracking of hexadecane with iron sulfide for 45 minutes at 420 °C

Compound	**Iron Sulfide, Water (mol%)**			**Iron Sulfide, No Water (mol%)**		
CH_4	8.39%	±	0.36%	9.09%	±	0.37%
CO_2	1.66%	±	0.19%	1.38%	±	0.74%
C_2H_4	4.92%	±	0.17%	4.78%	±	0.60%
C_2H_6	24.48%	±	0.84%	25.11%	±	3.09%
H_2S	0.06%	±	0.02%	0.00%	±	0.00%
C_3H_6	14.28%	±	0.37%	15.05%	±	0.46%
C_3H_8	14.94%	±	0.37%	16.80%	±	0.86%
1-C_4H_8	5.67%	±	0.16%	5.39%	±	0.44%
C_4H_{10}	7.07%	±	0.13%	7.07%	±	0.66%
2-C_4H_8	0.37%	±	0.17%	0.28%	±	0.07%
C_5+	17.14%	±	2.56%	13.88%	±	0.39%
CO	1.01%	±	0.17%	1.16%	±	0.41%

Previous studies have shown that through the use of n-dodecylsulfide, alkyl sulfides initiate liquid phase cracking due to the increase in labile bonds.[23] Initiation, by the decomposition of sulfide bonds, prevented the comparison of the conversion of the hexadecane to those cases without dimethyl disulfide. Instead, a series of runs were completed using FeS rather than α-Fe_2O_3 to observe the effect of iron sulfides on the liquid phase cracking of hexadecane. By comparison, in the absence of water the conversion of hexadecane is 24.2 ± 1.5% with α-Fe_2O_3, but only 15.3 ± 2.95% with FeS. Furthermore when water is added the conversion of hexadecane is reduced to 12.6 ± 2.0%, which is statistically equivalent to the conversion of hexadecane without water or catalyst. These results seem to indicate that FeS is less catalytically active then α-Fe_2O_3. In addition to the conversion, the alkane to alkene ratio in the presence of FeS is also depressed compared to that of α-Fe_2O_3 (Figure 4-10).

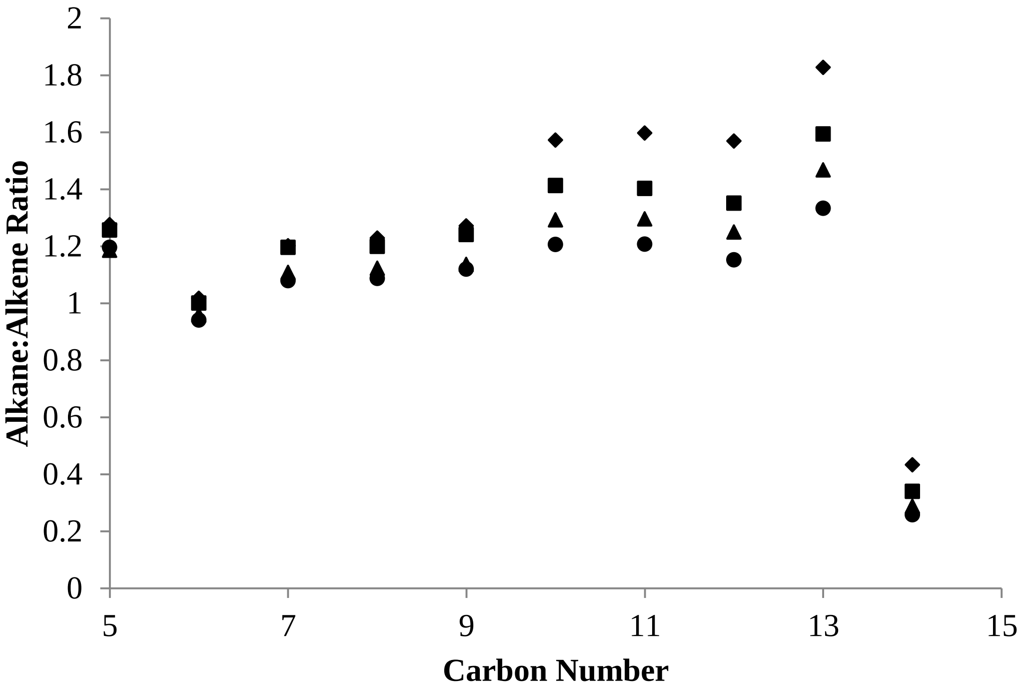

Figure 4-10. Alkane to Alkene ratio of produced liquid following the cracking of hexadecane with iron sulfide at 420 °C for 45 minutes in the presence or absence of steam(■-Iron Sulfide, No Water, ●-No Catalyst, No Water, ▲-Iron Sulfide, Water, ♦ - Hematite, Water)

Although it cannot be confirmed, it is thought that the main cause of the difference in both the conversion as well as the alkane to alkene ratio is the surface area of the catalyst. The surface area of the α-Fe_2O_3 is 3.352±0.056 m^2/g while FeS has a surface area of 0.217±0.001 m^2/g. This lower surface area also means a lower number of acid sites, explaining the lower conversion. In addition, the lower surface area also means the ratio of accessible acid sites to water molecules is decreased, causing the conversion to be statistically equivalent to the non-catalytic cases.

4.3 Effect of α-Fe_2O_3 and steam on the cracking of Cold Lake bitumen

The upgrading of bitumen via carbon rejection produces a large amount coke rich in heteroatoms which reduces its value and lowering the overall feed efficiency. Unfortunately, the pathway of highly aromatic sulfur likely cannot be changed without the use of energy intensive hydrodesulphurization processes, and will constantly lead to coke with a high heteroatom content. As shown earlier, α-Fe_2O_3 is capable of catalytically cracking hexadecane and reacting with hydrogen sulfide to produce iron sulfides, while the addition of water inhibits the formation of C_{16}+ products. It is therefore worth examining whether, the use of steam and α-Fe_2O_3 can decrease the coke yield during the cracking of Cold Lake bitumen, while simultaneously increasing the sulfur content of the resulting solids. Figure 4-11, 4-12 and 4-13 present the coke, liquid and gas yields as a function of residence time, respectively. At a residence time of 60 and 120 minutes the coke and liquid yields are equivalent for the cracking of bitumen with and without α-Fe_2O_3. On the other hand, when one looks at the effect of the steam on the decomposition of bitumen, a statistical difference in coke yield between the cases with and without water is observed. For all runs without water, the reactor was closed at a pressure of 5000 kPa, while for all runs with water, the reactor was closed at atmospheric pressure. Different initial pressures were used to account for the partial pressure of the steam at the reaction temperature. Therefore, the observed decrease in coke yield is due to the water and not simply an artifact caused by a pressure difference. By examining the interaction between α-Fe_2O_3 and water using two-way analysis of variance, the null hypothesis that the two additives have no interaction cannot be rejected. This does not imply that the null hypothesis is correct, simply that it cannot be rejected. Finally, the gas yield is equivalent for all the cases except for when the bitumen is thermally cracked without the addition of water or α-Fe_2O_3.

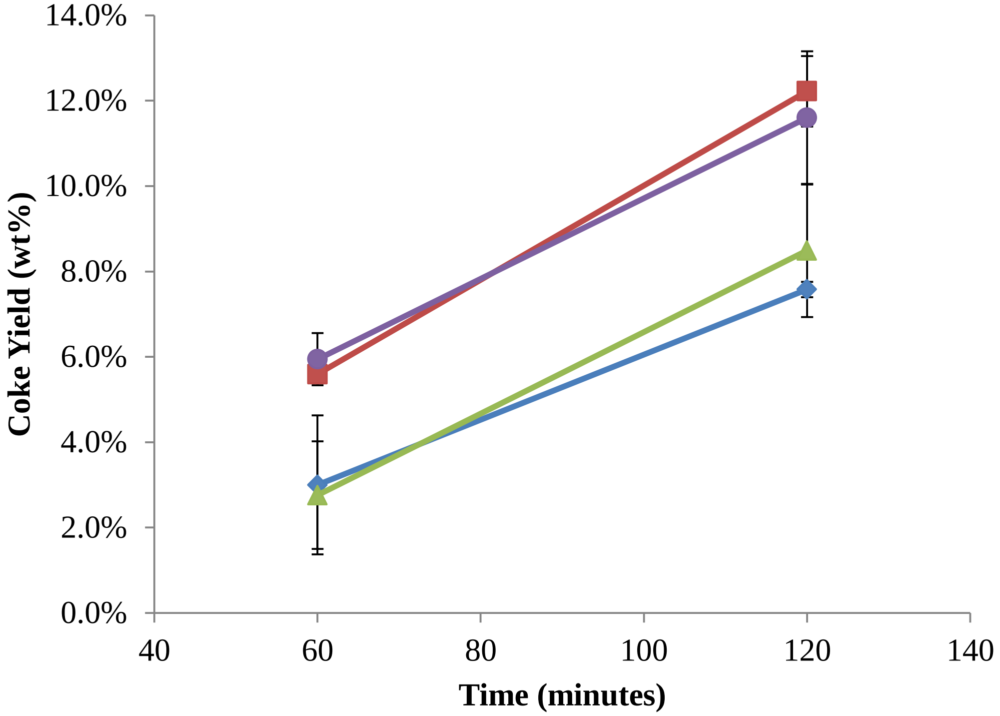

Figure 4-11. Coke yield as a function of time following the cracking of cold lake bitumen (■-α-Fe_2O_3, No Water, ●-No Catalyst, No Water, ▲-No Catalyst, Water, ♦ - α-Fe_2O_3, Water)

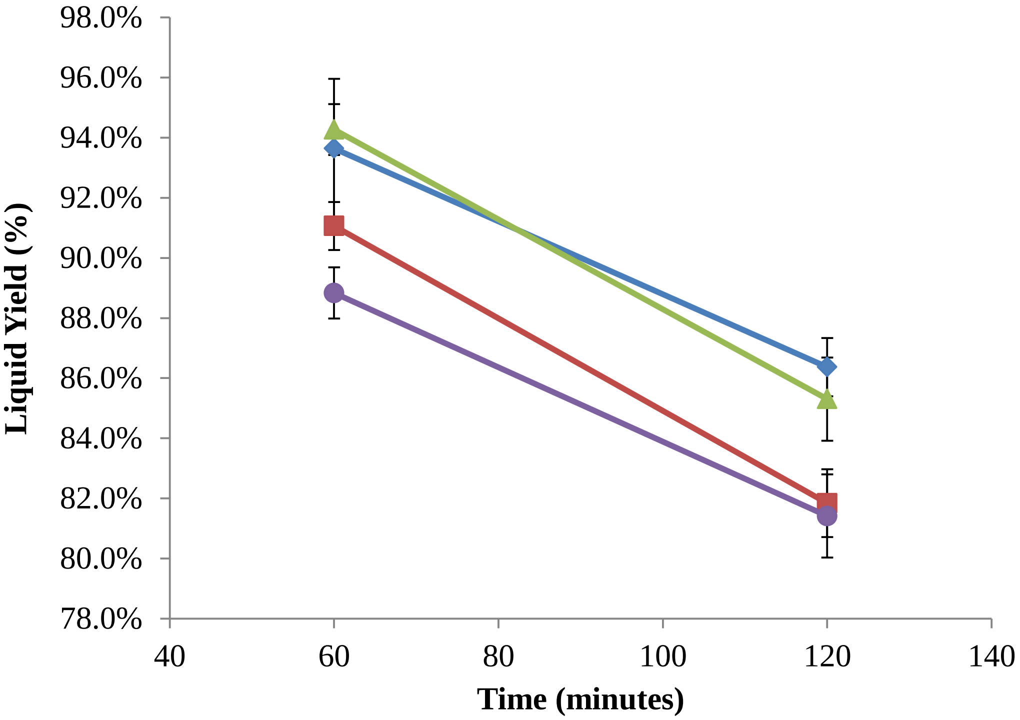

Figure 4-12. Liquid yield as a function of time following the cracking of cold lake bitumen (■-α-Fe_2O_3, No Water, ●-No Catalyst, No Water, ▲-No Catalyst, Water, ♦ - α-Fe_2O_3, Water)

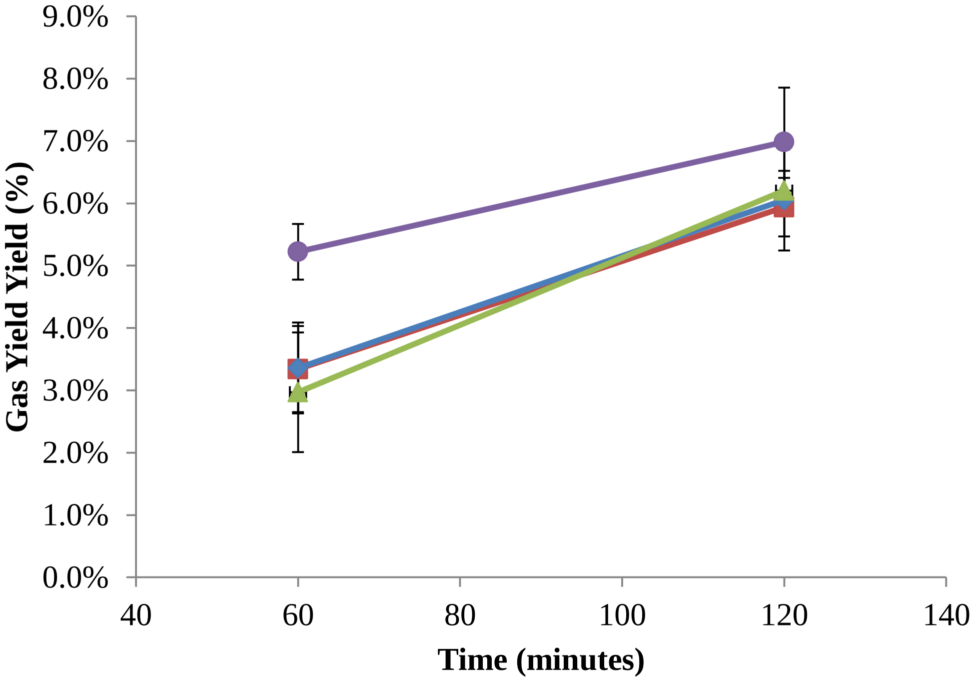

Figure 4-13. Gas yield as a function of time following the cracking of cold lake bitumen (■-α-Fe_2O_3, No Water, ●-No Catalyst, No Water, ▲-No Catalyst, Water, ♦ - α-Fe_2O_3, Water)

During the cracking of hexadecane, the use of α-Fe_2O_3 caused an increase in both the conversion and the fraction of addition products, however, the addition of water caused a decrease in both these. Furthermore, hydrogen sulfide is also known to react with the active sites, but this reaction is also inhibited by the presence of water. The inhibition of the reaction between the active sites and both the hydrocarbon and hydrogen sulfide due to the presence of water demonstrates the importance of competitive adsorption in the system. As Figure 4-14 presents, in the absence of water, hydrocarbons are free to interact with the active sites. However, by adding water the hydrocarbons must now compete with the water to interact with the active sites. Similar results were also expected when bitumen was fed to the system with the hypothesis that bitumen cracked with α-Fe_2O_3 should have an increased coke yield, while the addition of water would slightly reduce the coke yield during cracking with α-Fe_2O_3. As Figure 4-11 and 4-12 indicated, when thermally cracked bitumen is compared to bitumen cracked in the presence of α-Fe_2O_3, the yield of both coke and liquid products is equivalent, implying that α-Fe_2O_3 is not active in the catalytic cracking of bitumen. Furthermore, by adding water, a significant decrease in the coke yield was observed, however, unlike with hexadecane, no significant interaction between the α-Fe_2O_3 and the water was observed. The lack of any significant interaction implies that a second mechanism in addition to competitive adsorption is occurring. During the cracking of hexadecane, the surface of the catalyst and acid sites were easily accessible for hydrocarbons leading to an increased conversion. However, when switched to bitumen, the formation of coke on the surface of the catalyst (fouling) inhibits adsorption on to the active sites leading to the α-Fe_2O_3 having a negligible effect (Figure 4-14).

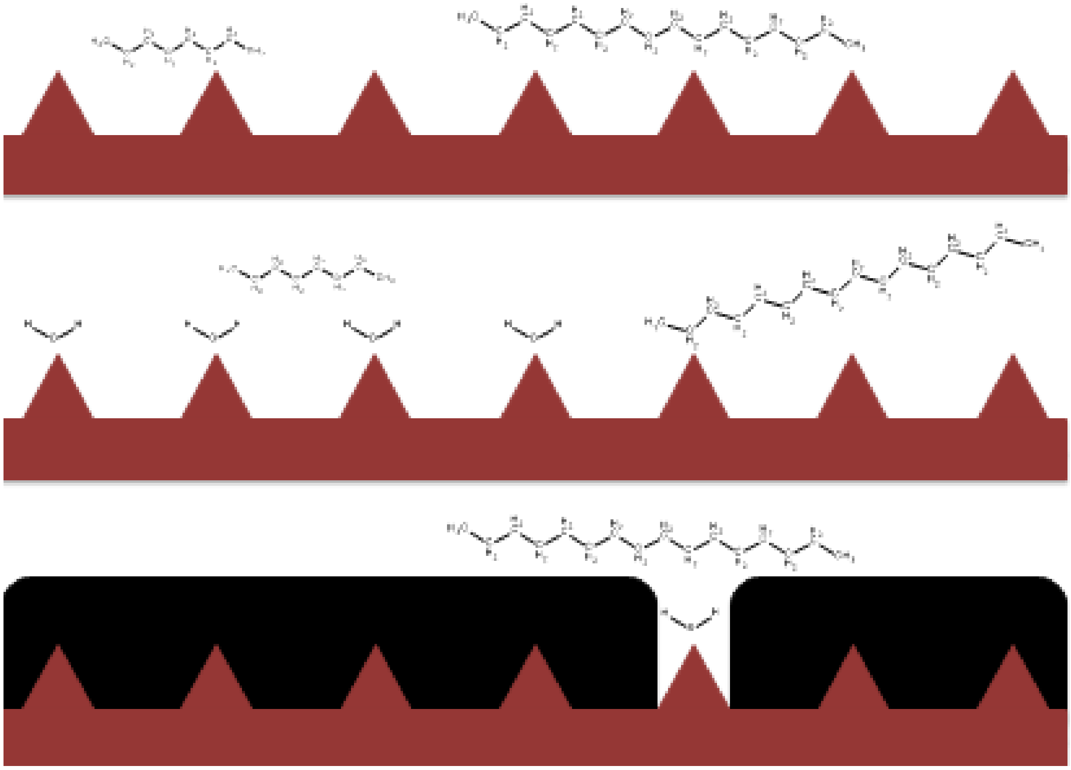

Figure 4-14. Graphical representation of interaction of hydrocarbons with active sites (triangles) on the surface of α-Fe_2O_3. Top: Adsorption of hydrocarbons on active sites in the absence of water. Middle: Competitive adsorption between hydrocarbons and water. Bottom: Fouling of catalyst by coke preventing larger hydrocarbons from interacting with active sites.

The decrease in coke yield in the presence of water is consistent with that found in literature,[3, 4, 90] while the impact of α-Fe_2O_3, or lack thereof, is contrary to that reported in the literature.[8-11] Clark and Kirk[4] used Iron(II)Sulfate, as opposed to α-Fe_2O_3, and attributed this reduction in coke yield to the coupling of the Fe(II)-Fe(III) system with improved electron transfer. The difference between the two systems may be attributed to the fact that once reduced to Fe_3O_4, it is thermodynamically impossible to produce Fe_2O_3 with steam[63] which, would limit any coupling between the two reactions. Fumoto *et al.*[8-11] developed a ZrO_2-Al_2O_3-Fe_2O_3 catalyst and found that when used with steam to crack various feed materials (including bitumen), a reduction in the insoluble solids formation resulted. It should be pointed out that this study and those completed by Fumoto *et al*. have a very different set-up. For this study a catalyst to bitumen ratio of 1:10 was used, while Fumoto *et al*. had a significantly more solids with a ratio ranging from 1:2.5 to 1:0.28.[11] Numerous studies have looked at the role of solids in the formation of coke and have concluded that solids do[5-7] and do not[5, 24, 91] lead to a reduction in the yield of coke. In general, it is agreed that any reduction in the insoluble solids yield is likely due to the solids collecting at the oil-coke interface and preventing coalescence of the coke.[6] This implies that any increase in solids concentration would also lead to a decrease in coke yield. Furthermore, it is predicted that by increasing the initial solids concentration, Fumoto *et al.*[11] is effectively reducing the impact of fouling by increasing the time needed to completely foul all the catalyst. Finally, it is also known that increasing the amount of water leads a reduction in the coke yield.[10, 90] Again the set-up of these experiments differ, where this study has a water to bitumen ratio of 1:5, Fumoto *et al*. typically used in the 1:0.315 range. Given the vast difference in the set-up, the results of Fumoto *et al.*[8-11] cannot be discounted. However, under the conditions used the use of α-Fe_2O_3 did not impact the coke yield.

Although α-Fe_2O_3 did not impact the coke yield, it did cause a statistical difference in the gas yield. As Figure 4-13 demonstrates, after a residence time of

60 minutes, the gas yield is equivalent for all cases except for when no water or α-Fe_2O_3 is present. This could be attributed to the inhibition of free radical reactions, however, as Tanabe and Gray[6] pointed out, any decrease in gas yield would require a decrease in coke yield as well. Furthermore, during the pyrolysis of coal tar pitch, the addition of $FeCl_3$ initiates mesophase formation via its Lewis acid sites,[24] which is consistent with the results obtained using hexadecane where an increase in conversion as well as addition products were observed due to the presence of acid sites. However, evidence of this would be an increase in the coke and gas yield and a decrease in liquid yield, none of which was seen.

The molar gas composition following the cracking of bitumen for 60 and 120 minutes is shown in Tables 4-3 and 4-4, respectively. At both residence times the concentration of carbon dioxide is higher in the presence of α-Fe_2O_3, while the concentration of carbon monoxide is statistically lower, implying that carbon monoxide is being oxidized by α-Fe_2O_3. Secondly, both Table 4-3 and 4-4 show a decrease in the H_2S concentration during the cracking with α-Fe_2O_3 and without water. The decrease in the H_2S concentration indicates that a similar reaction to that seen during the cracking of hexadecane is occurring resulting in the likely formation of iron sulfides.

Table 4-3. Gas phase molar composition following cracking of Cold Lake bitumen for 60 minutes (Fe=α-Fe_2O_3, NC= No Catalyst, NW=No Water, W= Water)

	Fe, NW (mol%)	NC, NW (mol%)	NC, W (mol%)	Fe, W (mol%)
CH_4	32.3% ± 0.5%	31.4% ± 1.1%	30.6% ± 1.1%	30.0% ± 1.0%
CO_2	4.3% ± 0.1%	2.9% ± 0.1%	3.9% ± 0.7%	3.9% ± 0.4%
C_2H_4	0.7% ± 0.0%	0.5% ± 0.0%	2.1% ± 0.1%	2.2% ± 0.1%
C_2H_6	16.8% ± 0.2%	16.1% ± 0.6%	13.4% ± 0.7%	13.4% ± 0.6%
H_2S	0.1% ± 0.1%	8.0% ± 0.8%	11.6% ± 2.2%	8.9% ± 2.8%
C_3H_6	2.4% ± 0.1%	2.0% ± 0.2%	4.9% ± 0.1%	4.9% ± 0.0%
C_3H_8	11.9% ± 0.1%	11.3% ± 0.2%	9.0% ± 0.3%	9.0% ± 0.4%
C_4	10.1% ± 0.1%	9.0% ± 0.3%	9.1% ± 0.1%	9.3% ± 0.6%
C_5	15.6% ± 0.4%	14.1% ± 0.4%	10.3% ± 0.8%	11.7% ± 1.4%
C_6	4.1% ± 0.1%	3.6% ± 0.1%	2.5% ± 0.7%	3.3% ± 0.5%
H_2	0.0% ± 0.0%	0.0% ± 0.0%	0.0% ± 0.0%	0.0% ± 0.0%
CO	1.7% ± 0.1%	1.2% ± 0.3%	2.7% ± 0.4%	3.6% ± 0.2%

Table 4-4. Gas phase molar composition following cracking of Cold Lake bitumen for 120 minutes

	Fe, NW (mol%)	NC, NW (mol%)	NC, W (mol%)	Fe, W (mol%)
CH_4	39.1% ± 0.8%	38.0% ± 1.2%	34.6% ± 3.2%	33.9% ± 1.6%
CO_2	3.3% ± 0.4%	2.1% ± 0.3%	2.7% ± 0.2%	3.3% ± 0.1%
C_2H_4	0.4% ± 0.0%	0.3% ± 0.0%	1.8% ± 0.6%	2.3% ± 0.1%
C_2H_6	19.7% ± 0.3%	18.8% ± 0.5%	15.9% ± 1.4%	15.4% ± 0.3%
H_2S	0.0% ± 0.0%	6.0% ± 0.8%	7.3% ± 1.2%	6.4% ± 0.3%
C_3H_6	1.3% ± 0.1%	1.1% ± 0.0%	3.9% ± 1.0%	4.7% ± 0.1%
C_3H_8	12.2% ± 0.3%	11.6% ± 0.2%	9.8% ± 1.2%	9.0% ± 0.3%
C_4	7.9% ± 0.5%	7.4% ± 0.1%	8.2% ± 0.7%	8.4% ± 0.5%
C_5	11.9% ± 1.4%	10.9% ± 1.0%	10.8% ± 1.8%	10.5% ± 1.0%
C_6	2.8% ± 0.2%	2.8% ± 0.2%	2.9% ± 0.8%	2.8% ± 0.3%
H_2	0.0% ± 0.0%	0.0% ± 0.0%	0.0% ± 0.0%	0.0% ± 0.0%
CO	1.3% ± 0.2%	1.0% ± 0.3%	2.2% ± 0.4%	3.2% ± 0.5%

It should be noted that in the presence of water, the alkane to alkene ratio decreases, regardless of the presence of α-Fe_2O_3, and leads to the theory that water is activating a mechanism and favoring the development of alkenes. During the cracking of hexadecane, a similar decrease in the alkane to alkene ratio upon the addition of water was observed within the gas fraction, however, the change in that ratio was minor compared to that observed within the bitumen system. It is possible that the result is simply an artifact of the water promoting the reaction between the hydrocarbons and the walls of the reactor and, had a reactor with a larger volume to surface area been used, no change in the alkane to alkene ratio would have been observed. In addition to the wall effects, given the large difference between the hexadecane and bitumen systems, is seems more plausible that this result is due to either the different amounts of water added to the system (5 wt% vs. 20 wt%) or a due to the feed. It has previously been reported that the associated bitumen solids are capable of acting as catalysts in the presence of hydrogen[92] and although it cannot be confirmed, it is hypothesized that the addition of water to the bitumen system, may be activating the associated solids causing the change in the alkane to alkene ratio.

The cracking of hexadecane indicated that more CO_2 was produced with α-Fe_2O_3, while the addition of water did not change the yield of carbon oxides produced. By comparison, when bitumen is degraded for 60 minutes, the concentration of CO_2 is equivalent regardless of the additives. This can be explained from the fact that hexadecane has no associated oxygen, while the bitumen contains 1.54% oxygen. On the other hand, at a residence time of 120 minutes (Table 4-4), more CO_2 appears to be produced when α-Fe_2O_3 is present. By using the mass of gas produced and converting Table 4.4 into mass percent, the total mass of CO_2 produced for all four runs was calculated. If the mass of CO_2 produced from the bitumen is assumed to be the average of the runs involving no catalyst, then the total mass of CO_2 produced by α-Fe_2O_3 can be calculated to be less 1% of the total gas produced. Thus, similar to the model compound study, the oxidation of bitumen by α-Fe_2O_3 is a minor reaction pathway.

While the formation of carbon dioxide by the reduction of α-Fe_2O_3 appears to be a minor reaction route, the same cannot be said for the adsorption and subsequent reaction of H_2S. As Tables 4-3 and 4-4 show, at both residence times the addition of α-Fe_2O_3 leads to a significant reduction in the yield of H_2S. This is expected to follow a similar to pathway to that seen with hexadecane, where the H_2S concentration decreased but the iron oxide became sulfided. Table 4-5 displays the normalized elemental weight compositions of the solid particles. The Elementar Vario Microcube elemental analyzer is only capable of directly measuring the concentration of the carbon, hydrogen, nitrogen and sulfur within a compound, with the oxygen content of a hydrocarbon sample typically being calculated by difference. This causes a problem for any sample initially containing α-Fe_2O_3 as the presence of iron makes it impossible to calculate the oxygen content. Therefore, the data presented is normalized and displays the weight percent of each element as if only these four elements were present. As expected, the solids containing α-Fe_2O_3 have a significantly higher concentration of sulfur than the non-catalytic cases, with the addition of water again inhibiting the formation of sulfur rich solids, implying a similar mechanism to that seen with hexadecane. Due to coke formation on the catalyst, an XRD pattern could not be measured. However, it is expected that the structure will be close to pyrrhotite, which was observed following the cracking of coal liquids with hematite and steam at milder conditions.[64]

Table 4-5. Normalized elemental weight composition of insoluble solids following cracking of Cold Lake bitumen for 60 and 120 minutes* (NC=No Catalyst, Fe= α-Fe_2O_3, W= Water, NW = No Water)

Residence time (min)	Run	Carbon (wt%)	Hydrogen (wt%)	Sulfur (wt%)	Nitrogen (wt%)	Atomic H/C Ratio
60	Fe, NW	68.5	4.4	24.0	3.2	0.764
	NC, NW	82.8	4.7	9.8	2.7	0.675
	NC, W	82.0	5.5	9.0	3.4	0.798
	Fe, W	70.2	5.6	17.4	6.8	0.949
120	Fe, NW	76.8	4.2	16.6	2.4	0.650
	NC, NW	84.9	4.6	8.0	2.4	0.644
	NC, W	85.2	4.5	7.8	2.6	0.628
	Fe, W	80.0	4.8	12.2	3.0	0.713

*Normalized due to inability to remove measure concentration of Fe or O

As mentioned earlier, the majority of coke is stockpiled at mine sites[2] as its value is significantly reduced due to its high heteroatom content, accounting for a large loss of potential product. Thus, it was hoped that the cracking of bitumen under the conditions of this study would lead to a decrease in coke formation, increased sulfur content and a lower H/C ratio. As we have seen, water leads to a reduction in coke formation but inhibits the adsorption of sulfur species by α-Fe_2O_3. Furthermore, as Table 4-5 shows the addition of α-Fe_2O_3 or water leads an increase in the H/C ratio with the highest H/C ratio resulting from the addition of both α-Fe_2O_3 and water. An increase in the H/C ratio is an indication of a decrease in the H/C ratio in the liquid. Although the carbon, hydrogen, nitrogen and sulfur content of the liquid was measured only the sulfur and nitrogen content can be taken as accurate because, during the extraction process toluene was used as a solvent. Unfortunately the complete removal of toluene could not be obtained resulting in the carbon and hydrogen content of the liquid being skewed. As a result, it is concluded that the use of α-Fe_2O_3 and water does not lead to a decrease in both the coke yield and H/C ratio.

From Tables 4-3, 4-4 and 4-5 it appears that the α-Fe_2O_3 is reacting with H_2S to form FeS, via a similar mechanism to that observed with hexadecane and DMDS. To confirm, a sulfur balance was completed (Table 4-6) and shows the mass of sulfur in the gas, liquid and solid for the four conditions following cracking at 420 °C for 60 minutes, with each run being the average of triplicate runs. Also included in Table 4-6 is the mass of the sulfur within the solids for a residence time of 120 minutes. As expected, cracking bitumen with α-Fe_2O_3 and no water resulted in the gas containing approximately 100 times less hydrogen sulfide than any other case, and almost double the amount of sulfur in the solid. However, when the sulfur in the liquid is analyzed it is found that all samples contain statistically equivalent quantities of sulfur.

Table 4-6. Sulfur Balance following cracking of Cold Lake bitumen at 420 °C for 60 minutes (NC=No Catalyst, Fe= α-Fe_2O_3, W= Water, NW = No Water)

Run	$m_{g,s,60}$ (g)	$m_{l,s,60}$ (g)	$m_{c,s,60}$ (g)	Mass of Sulfur (g)	Recovered (%)	$m_{c,s,120}$ (g)
Fe, NW	8.53×10^{-5}	1.22×10^{-1}	4.09×10^{-2}	1.63×10^{-1}	104.2	6.31×10^{-2}
NC, NW	9.95×10^{-3}	1.24×10^{-1}	1.42×10^{-2}	1.48×10^{-1}	95.1	2.63×10^{-2}
NC, W	1.43×10^{-2}	1.27×10^{-1}	3.83×10^{-3}	1.45×10^{-1}	92.9	1.72×10^{-2}
Fe, W	1.02×10^{-2}	1.28×10^{-1}	1.13×10^{-2}	1.49×10^{-1}	95.6	2.60×10^{-2}

Before the sulfur balance can be discussed further, it must be pointed out that the total sulfur recovered is never exactly 100% which can be attributed to two factors:

1. The total gas yield is 3%-5.2% of the feed. Given that only 3 g of feed is used, a 1% difference corresponds to only 0.03 g and thus if any sand, water or particulate is left on the reactor a significant error in the gas yield will be induced. This causes the gas yield to be the least accurate of all measurements.
2. A fraction of the hydrogen sulfide will be dissolved in the liquid product. The liquid and solid products are extracted from the reactor using toluene. The toluene is removed from the liquid product by rotary evaporation at a pressure of 77 mBar and a temperature of 60 °C. Therefore, during the rotary evaporation, any hydrogen sulfide in the liquid will be lost.

As mentioned, the total sulfur in the liquid products is equivalent under all four conditions. This equivalent sulfur content is due to the aromatic sulfur, such as thiophene, being stable under the reaction conditions.[17] Due to the stable nature of aromatic sulfur compounds, it must be assumed that, the sulfur moving from the gas to the solids is H_2S. By comparing the two cases with no water and a residence time of 60 minutes, the difference in sulfur content of the solids is 0.0267 g, while the difference in the sulfur content of the gas is only 0.0099 g. If only the location of the sulfide sulfur is changing and the sulfur content of the liquids is equivalent, then it is required that the differences in the mass of sulfur in the gas and solid should be equivalent. This is obviously not the case, but can be explained by the fact that the sulfur lost during rotary evaporation is only lost by the non-catalytic case, as any H_2S formed during the reaction, including that dissolved in the liquid, would have been absorbed by α-Fe_2O_3. Previous research has found that 1.25% of the feed bitumen is sulfur in sulfide structures.[67] At a residence time of 60 minutes for the case involving α-Fe_2O_3 and no water, the increase in the sulfur content of the solids is equivalent to 0.88% of the feed, indicating the not all of the sulfides have broken down to H_2S. At 120 minutes, if it is assumed that the increase in the mass of sulfur is due to the reaction of sulfides, the sulfur contained within sulfide bonds can be calculated to be 1.23%, which is in line with previous studies and indicates that all the sulfide sulfur has been broken down to H_2S. The increasing amount of sulfides reacting with the catalyst is important as it shows that even though fouling is occurring, smaller molecules such as hydrogen sulfide can still move through the coke pores and react with the iron oxide, as previously shown in Figure 4-14. Furthermore, by comparing the mass of sulfur within the solid at 60 minutes to that at 120 minutes, it can be seen that the greatest increase in sulfur content is for the case involving α-Fe_2O_3 followed by the α-Fe_2O_3-water case. The fact that adding water again inhibits the reaction between hydrogen sulfide and the iron oxide indicates that competitive adsorption is ongoing even after the catalyst has undergone fouling.

Similar to the model compound study, the incorporation of water into the reaction system inhibited the formation of iron sulfides and resulted in a coke with a lower sulfur content than the system involving only α-Fe_2O_3. Contrary to the model compound study, the addition of α-Fe_2O_3 did not affect the decomposition of bitumen, or the coke yield. Although a decrease in the coke yield was observed in the presence of both water and α-Fe_2O_3 the decreased yield was equivalent to the case involving only water and thus the α-Fe_2O_3 had no effect. Therefore, the simultaneous use of α-Fe_2O_3 and water does not provide the conditions looked for to make this a suitable pathway to explore further.

Chapter 5: Conclusions

The liquid phase decomposition of n-hexadecane and Cold Lake bitumen has been studied in the presence and absence of steam and α-Fe_2O_3. The use of different feeds highlighted the importance of both competitive adsorption and fouling of the catalyst. The catalytic cracking of hexadecane indicated that α-Fe_2O_3 possesses some catalytic cracking ability resulting in an increased conversion and alkane to alkene ratio. The increase in the alkane to alkene ratio has been primarily contributed to the addition of carbenium ions to the alkenes, due to an increase in the addition products. The absence of any short chain branched alkanes indicated that the increased alkane to alkene ratio was not due to the disproportiation reaction. Adding steam to the reaction medium caused no change in the decomposition of hexadecane in the absence of α-Fe_2O_3. By comparison, when α-Fe_2O_3 and steam were both present, the conversion and alkane to alkene ratio both decreased compared to when steam was absent. The decrease in these catalytic indicators were attributed to water inhibiting the interaction of the surface with the hydrocarbons by two mechanisms. First, water can hydrogen bond with surface hydroxyl groups and thus sterically inhibit the interaction of the hydrocarbon with the Bronsted sites. Secondly, acting as a Lewis base, the water can donate its lone pair of electrons to the Lewis acids resulting in the molecular adsorption of water on the surface and highlighting the importance of competitive adsorption to the α-Fe_2O_3-water system.

To investigate the role of sulfur in the liquid phase thermal cracking of hexadecane, dimethyl disulfide was added to the feed. The decomposition of dimethyl disulfide resulted in the formation of hydrogen sulfide which was shown to react with the iron oxide to produce iron sulfide. Similar to the decomposition of hexadecane, the reaction of hydrogen sulfide and α-Fe_2O_3 was inhibited due to competitive adsorption with the steam, resulting in a greater hydrogen sulfide concentration and a decreased sulfur concentration within the iron oxide. The impact of iron sulfide was studied by cracking hexadecane with FeS and resulted in an alkane to alkene ratio greater than that of thermal cracking, but depressed when compared to the case involving α-Fe_2O_3. Furthermore, the addition of steam again depressed the catalytic cracking indicators producing a conversion and alkane to alkene ratio statistically equivalent to thermal cracking. In addition to competitive adsorption, the formation of hydrogen sulfide in the reaction of steam and FeS, confirmed that water also oxidizes FeS.

α-Fe_2O_3 was concluded to be catalytically active towards cracking. However, when the feed was Cold Lake bitumen no catalytic cracking ability was noticed regardless of the presence or absence of steam. Both the gas and coke yields were expected to increase in the presence of α-Fe_2O_3, however, neither did, leading to the conclusion that fouling of the catalyst was occurring and blocking the active sites. Fouling only prevented interactions between the active sites and larger molecules as the α-Fe_2O_3 still reacted with hydrogen sulfide to produce a solid rich in sulfur. The introduction of steam to the α-Fe_2O_3 system proved that competitive adsorption was still occurring and resulted in the produced solid having a sulfur content lower than that of the case with only α-Fe_2O_3. Therefore, it is concluded that α-Fe_2O_3 does possess some catalytic ability. This catalytic ability is inhibited by fouling of the catalyst and by the adsorption of water on the active sites. Thus, negating the simultaneous use of steam and α-Fe_2O_3 to decrease coke yield, while increasing the sulfur content of the solid.

Chapter 6: References

---

(1) Junaid, A. S. M.; Yin, H.; Koenig, A.; Swenson, P.; Chowdhury, J.; Burland, G.; McCaffrey, W. C.; Kuznicki, S. M. Natural zeolite catalyzed cracking-assisted light hydrocarbon extraction of bitumen from Athabasca oilsands. *Appl. Catal., A* **2009**, *354*, 44-49.

(2) Gray, M. R. *Fundamentals of Oil Sands Upgrading*, Couse Notes: CH E 522. **2008**, pp. C5-5 - C5-24.

(3) Dutta, R. P.; McCaffrey, W. C.; Gray, M. R.; Muehlenbachs, K. Thermal cracking of Athabasca bitumen: Influence of steam on reaction chemistry. *Energy Fuels* **2000**, *14*, 671-676.

(4) Clark, P. D.; Kirk, M. J. Studies on the Upgrading of Bituminous Oils with Water and Transition-Metal Catalysts. *Energy Fuels* **1994**, *8*, 380-387.

(5) Sanaie, N.; Watkinson, A. P.; Bowen, B. D.; Smith, K. J. Effect of minerals on coke precursor formation. *Fuel* **2001**, *80*, 1111-1119.

(6) Tanabe, K.; Gray, M. R. Role of fine solids in the coking of vacuum residues. *Energy Fuels* **1997**, *11*, 1040-1043.

(7) Rahimi, P.; Gentzis, T.; Fairbridge, C. Interaction of clay additives with mesophase formed during thermal treatment of solid-free Athabasca bitumen fraction. *Energy Fuels* **1999**, *13*, 817-825.

(8) Fumoto, E.; Tago, T.; Tsuji, T.; Masuda, T. Recovery of useful hydrocarbons from petroleum residual oil by catalytic cracking with steam over zirconia-supporting iron oxide catalyst. *Energy Fuels* **2004**, *18*, 1770-1774.

(9) Fumoto, E.; Tago, T.; Masuda, T. Production of lighter fuels by cracking petroleum residual oils with steam over zirconia-supporting iron oxide catalysts. *Energy Fuels* **2006**, *20*, 1-6.

(10) Fumoto, E.; Matsumura, A.; Sato, S.; Takanohashi, T. Recovery of Lighter Fuels by Cracking Heavy Oil with Zirconia-Alumina-Iron Oxide Catalysts in a Steam Atmosphere. *Energy Fuels* **2009**, *23*, 1338-1341.

(11) Fumoto, E.; Sato, S.; Takanohashi, T. Production of Light Oil by Oxidative Cracking of Oil Sand Bitumen Using Iron Oxide Catalysts in a Steam Atmosphere. *Energy Fuels* **2011**, *25*, 524-527.

(12) Garg, D.; Tarrer, A. R.; Guin, J. A.; Curtis, C. W.; Clinton, J. H. Selective Action of Hematite in Coal Desulfurization. *Ind. Eng. Chem. Process Des. Dev.* **1980**, *19*, 572-580.

(13) Sasaoka, E.; Ichio, T.; Kasaoka, S. High-Temperature H_2S Removal from Coal-Derived Gas by Iron-Ore. *Energy Fuels* **1992**, *6*, 603-608.

(14) Saniere, A. Definitions and Specificities. In *Heavy Crude Oils: From Geology to Upgrading an Overview;* Huc, A. Y., Ed.; Editions Technip: France, 2011; pp 12-13

(15) Maples, R. E. *Petroleum Refinery Process Economics*, 2nd ed.; PennWell: Online, 2000, http://www.knovel.com/web/portal/browse/display?_EXT_KNOVEL_DISPLAY_bookid=3617&VerticalID=0 (Accessed October 15, 2012)

(16) Strausz, O. P.; Lown, E. M. In *The Chemistry of Alberta Oil Sands, Bitumen and Heavy Oils;* Alberta Energy Research Institute: Calgary, 2003; pp 695.

(17) Gray, M. R. *Upgrading petroleum residues and heavy oils;* M. Dekker: New York, 1994; pp 348.

(18) Sawarkar, A. N.; Pandit, A. B.; Samant, S. D.; Joshi, J. B. Petroleum residue upgrading via delayed coking: A review. *Can. J. Chem. Eng.* **2007**, *85*, 1-24.

(19) Wiehe, I. A. A phase-separation kinetic model for coke formation. *Ind. Eng. Chem. Res* **1993**, *32*, 2447-2454.

(20) Brooks, J. D.; Taylor, G. H. Formation of graphitizing carbons from the liquid phase. *Nature* **1965**, *206*, 697-699.

(21) Rahmani, S.; McCaffrey, W.; Elliott, J. A. W.; Gray, M. R. Liquid-phase behavior during the cracking of asphaltenes. *Ind. Eng. Chem. Res* **2003**, *42*, 4101-4108.

(22) Bi, W. D.; McCaffrey, W. C.; Gray, M. R. Agglomeration and deposition of coke during cracking of petroleum vacuum residue. *Energy Fuels* **2007**, *21*, 1205-1211.

(23) Rahmani, S.; McCaffrey, W.; Gray, M. Kinetics of solvent interactions with asphaltenes during coke formation. *Energy Fuels* **2002**, *16*, 148-154.

(24) Alain, E.; Begin, D.; Furdin, G.; Mareche, J. F. Effect of graphite or $FeCl_3$-graphite intercalation compounds on the mesophase development in coal tar pitch. *Carbon* **1996**, *34*, 619-626.

(25) Masuda, T.; Kondo, Y.; Miwa, M.; Shimotori, T.; Mukai, S. R.; Hashimoto, K.; Takano, M.; Kawasaki, S.; Yoshida, S. Recovery of useful hydrocarbons from oil palm waste using ZrO_2 supporting FeOOH catalyst. *Chem. Eng. Sci.* **2001**, *56*, 897-904.

(26) Rice, F. The thermal decomposition of organic compounds from the standpoint of free radicals. I. Saturated hydrocarbons. *J. Am. Chem. Soc.* **1931**, *53*, 1959-1972.

(27) Rice, F.; Herzfeld, K. The thermal decomposition of organic compounds from the standpoint of free radicals VI The mechanism of some chain reactions. *J. Am. Chem. Soc.* **1934**, *56*, 284-289.

(28) Kossiakoff, A.; Rice, F. Thermal decomposition of hydrocarbons, resonance stabilization and isomerization of free radicals. *J. Am. Chem. Soc.* **1943**, *65*, 590-595.

(29) Voge, H. H.; Good, G. M. Thermal Cracking of Higher Paraffins. *J. Am. Chem. Soc.* **1949**, *71*, 593-597.

(30) Depeyre, D.; Flicoteaux, C.; Chardaire, C. Pure n-hexadecane thermal steam cracking. *Ind. Eng. Chem. Process Des. Dev.* **1985**, *24*, 1251-1258.

(31) Doue, F.; Guiochon, G. Formation of Alkanes in Pyrolysis of N-Hexadecane - Effect of an Inert Gas on Decomposition of Alkyl Radicals. *Can. J. Chem.* **1969**, *47*, 3477-3480.

(32) Rebick, C. Pyrolysis of Heavy Hydrocarbons. In *Pyrolysis: Theory and Industrial Practice*; Albright, L. F., Crynes, B. L. and Corcoran, W. H., Eds.; Academic Press: New York 1983; pp 71-78.

(33) Ford, T. J. Liquid-Phase Thermal-Decomposition of Hexadecane - Reaction-Mechanisms. *Ind. Eng. Chem. Fundamen* **1986**, *25*, 240-243.

(34) Wu, G.; Katsumura, Y.; Matsuura, C.; Ishigure, K.; Kubo, J. Comparison of Liquid-Phase and Gas-Phase Pure Thermal Cracking of n-Hexadecane. *Ind. Eng. Chem. Res* **1996**, *35*, 4747-4754.

(35) Safarik, I.; Strausz, O. P. The thermal decomposition of hydrocarbons. Part 1. n-alkanes ($C \geq 5$). *Res. Chem. Intermed.* **1996**, *22*, 275-314.

(36) Khorasheh, F.; Gray, M. R. High-Pressure Thermal-Cracking of N-Hexadecane. *Ind. Eng. Chem. Res.* **1993**, *32*, 1853-1863.

(37) Gray, M.; McCaffrey, W. Role of chain reactions and olefin formation in cracking, hydroconversion, and coking of petroleum and bitumen fractions. *Energy Fuels* **2002**, *16*, 756-766.

(38) Khorasheh, F.; Gray, M. R. High-pressure thermal cracking of n-hexadecane in aromatic solvents. *Ind. Eng. Chem. Res.* **1993**, *32*, 1864-1876.

(39) Blanksby, S. J.; Ellison, G. B. Bond dissociation energies of organic molecules. *Acc. Chem. Res.* **2003**, *36*, 255-263.

(40) Savage, P.; Klein, M. Asphaltene Reaction Pathways .2. Pyrolysis of N-Pentadecylbenzene. *Ind. Eng. Chem. Res.* **1987**, *26*, 488-494.

(41) Smith, C.; Savage, P. Reactions of Polycyclic Alkylaromatics .1. Pathways, Kinetics, and Mechanisms for 1-Dodecylpyrene Pyrolysis. *Ind. Eng. Chem. Res.* **1991**, *30*, 331-339.

(42) Corma, A.; Orchillés, A. V. Current views on the mechanism of catalytic cracking. *Microporous Mesoporous Mater.* **2000**, *35-36*, 21-30.

(43) Greensfelder, B. S.; Voge, H. H.; Good, G. M. Catalytic and Thermal Cracking of Pure Hydrocarbons - Mechanisms of Reaction. *Ind. Eng. Chem.* **1949**, *41*, 2573-2584.

(44) Kotrel, S.; Knözinger, H.; Gates, B. C. The Haag-Dessau mechanism of protolytic cracking of alkanes. *Microporous Mesoporous Mater.* **2000**, *35-36*, 11-20.

(45) Cumming, K.; Wojciechowski, B. Hydrogen transfer, coke formation, and catalyst decay and their role in the chain mechanism of catalytic cracking. *Catal. Rev. Sci. Eng.* **1996**, *38*, 101-157.

(46) Schmidt, R.; Welch, M. B.; Anderson, R. L.; Sardashti, M.; Randolph, B. B. Disproportionation of light paraffins. *Energy Fuels* **2008**, *22*, 1812-1823.

(47) Den Hollander, M. A.; Wissink, M.; Makkee, M.; Moulijn, J. A. Gasoline conversion: Reactivity towards cracking with equilibrated FCC and ZSM-5 catalysts. *Appl. Catal. A* **2002**, *223*, 85-102.

(48) Ferretto, L.; Glisenti, A. Study of the surface acidity of an hematite powder. *J. Mol. Catal. A-Chem.* **2002**, *187*, 119-128.

(49) Cornell, R. M.; Schwertmann, U. *The Iron Oxides: Structure, Properties, Reactions, Occurences and Uses;* Wiley-VCH: Weinheim, 2003

(50) Kohl, A. L.; Nielsen, R. B. *Gas Purification;* Elsevier: Houston, 1997; 1298-1305.

(51) Kung, H. *Transition Metal Oxides: Surface Chemistry and Catalysis;* Studies in Surface Science and Catalysis, Vol 45, Elsevier: New York, 1989; 53-90.

(52) Yamamoto, S.; Kendelewicz, T.; Newberg, J. T.; Ketteler, G.; Starr, D. E.; Mysak, E. R.; Andersson, K. J.; Ogasawara, H.; Bluhm, H.; Salmeron, M.; Brown, G. E., Jr.; Nilsson, A. Water Adsorption on alpha-Fe_2O_3(0001) at near Ambient Conditions. *J. Phys. Chem. C* **2010**, *114*, 2256-2266.

(53) Yin, S.; Ma, X.; Ellis, D. E. Initial stages of H_2O adsorption and hydroxylation of Fe-terminated alpha-Fe_2O_3(0001) surface. *Surf. Sci.* **2007**, *601*, 2426-2437.

(54) Lorenzelli, V.; Busca, G. Infrared Studies of the Surface of Alpha-Fe_2O_3. *Mater. Chem. Phys.* **1985**, *13*, 261-281.

(55) Dent, A. L.; Kokes, R. J. The nature of adsorbed propylene on zinc oxide. II. Reactions of π-allyl species. *J. Am. Chem. Soc.* **1970**, *92*, 6718-6723.

(56) Busca, G.; Zerlia, T.; Lorenzelli, V.; Girelli, A. Fourier Transform-Infrared Study of the Adsorption of Unsaturated and Aromatic-Hydrocarbons on the Surface of Alpha-Fe_2O_3 .2. Benzene. *J. Catal.* **1984**, *88*, 131-136.

(57) Busca, G.; Zerlia, T.; Lorenzelli, V.; Girelli, A. Fourier transform-infrared study of the adsorption of unsaturated and aromatic hydrocarbons on the surface of α-Fe_2O_3. I. Ethylene. *J. Catal.* **1984**, *88*, 125-130.

(58) Cypres, R.; Soudan-Moinet, C. Pyrolysis of coal and iron oxides mixtures. 1. Influence of iron oxides on the pyrolysis of coal. *Fuel* **1980**, *59*, 48-54.

(59) Brown, A. S. C.; Hargreaves, J. S. J.; Rijnierse, B. A study of the structural and catalytic effects of sulfation on iron oxide catalysts prepared from goethite and ferrihydrite precursors for methane oxidation. *Catal. Lett.* **1998**, *53*, 7-13.

(60) Scirè, S.; Minicò, S.; Crisafulli, C.; Galvagno, S. Catalytic combustion of volatile organic compounds over group IB metal catalysts on Fe_2O_3. *Catal. Commun.* **2001**, *2*, 229-232.

(61) Pineau, A.; Kanari, N.; Gaballah, I. Kinetics of reduction of iron oxides by H_2. Part I: Low temperature reduction of hematite. *Thermochim. Acta* **2006**, *447*, 89-100.

(62) Rydén, M.; Arjmand, M. Continuous hydrogen production via the steam-iron reaction by chemical looping in a circulating fluidized-bed reactor. *Int. J. Hydrogen Energy* **2012**, *37*, 4843-4854.

(63) Bleeker, M. F.; Kersten, S. R. A.; Veringa, H. J. Pure hydrogen from pyrolysis oil using the steam-iron process. *Catal. Today* **2007**, *127*, 278-290.

(64) Sharypov, V. I.; Kuznetsov, B. N.; Beregovtsova, N. G.; Baryshnikov, S. V.; Sidel'nikov, V. N. Steam cracking of coal-derived liquids and some aromatic compounds in the presence of haematite. *Fuel* **1996**, *75*, 791-794.

(65) Davydov, A.; Chuang, K.; Sanger, A. Mechanism of H_2S oxidation by ferric oxide and hydroxide surfaces. *J. Phys. Chem. B* **1998**, *102*, 4745-4752.

(66) Komraus, J. L.; Popiel, E. S. Chemical transformation of iron compounds during the process of coal pyrolysis in steam. *Hyperfine Interact.* **1994**, *90*, 383-388.

(67) Gray, M. R.; Ayasse, A. R. Kinetics of Hydrodesulfurization of Thiophenic and Sulfide Sulfur in Athabasca Bitumen. *Energy Fuels* **1995**, *9*, 500-506.

(68) Brons, G.; Yu, J. M. Solvent deasphalting effects on whole cold lake bitumen. *Energy Fuels* **1995**, *9*, 641-647.

(69) Greinke, R. A.; Lewis, I. C. Pyrolysis studies on model aromatic sulfur compounds. *Carbon* **1979**, *17*, 471-477.

(70) Vandeputte, A. G.; Reyniers, M.; Marin, G. B. Theoretical Study of the Thermal Decomposition of Dimethyl Disulfide. *J. Phys. Chem. A* **2010**, *114*, 10531-10549.

(71) Coope, J. A. R.; Bryce, W. A. The Thermal Decomposition of Dimethyl Disulphide. *Can. J. Chem.* **1954**, *32*, 768-779.

(72) Thompson, C. J.; Meyer, R. A.; Ball, J. S. Thermal decomposition of sulfur compounds. I. 2-Methyl-2-propanethiol. *J. Am. Chem. Soc.* **1952**, *74*, 3284-3287.

(73) Dietz, W. A. Response Factors for Gas Chromatographic Analyses. *J. of Gas Chromatography* **1967**, *5*, 68-71.

(74) Wojciechowski, B. The reaction mechanism of catalytic cracking: Quantifying activity, selectivity, and catalyst decay. *Catal. Rev. Sci. Eng.* **1998**, *40*, 209-328.

(75) Mills, P.; Sullivan, J. L. A Study of the Core Level Electrons in Iron and its 3 Oxides by Means of X-Ray Photoelectron-Spectroscopy. *J. Phys. D: Appl. Phys.* **1983**, *16*, 723-732.

(76) Junta-Rosso, J. L.; Hochella, M. F. The chemistry of hematite {001} surfaces. *Geochim. Cosmochim. Acta* **1996**, *60*, 305-314.

(77) Sie, S.T. Acid-Catalyzed Cracking of Paraffinic Hydrocarbons .1. Discussion of Existing Mechanisms and Proposal of a New Mechanism. *Ind. Eng. Chem. Res.* **1992**, *31*, 1881-1889.

(78) Bassir, M.; Wojciechowski, B. The Protolysis of Hexanes Over a USHY Zeolite. *J. Catal.* **1994**, *150*, 1-8.

(79) Cant, N. W.; Little, L. H. Lewis and Bronsted Acid Sites on Silica-Alumina. *Nature* **1966**, *211*, 69-70.

(80) Hendewerk, M.; Salmeron, M.; Somorjai, G. A. Water-Adsorption on the (001) Plane of Fe_2O_3 - an Xps, Ups, Auger, and Tpd Study. *Surf Sci* **1986**, *172*, 544-556.

(81) McCafferty, E.; Zettlemoyer, A.C. Adsorption of Water Vapor on Alpha-Fe2o3. *Discuss. Faraday Soc.* **1971**, 239-254.

(82) Joseph, Y.; Ranke, W.; Weiss, W. Water on FeO(111) and Fe_3O_4(111): Adsorption behavior on different surface terminations. *J. Phys. Chem. B* **2000**, *104*, 3224-3236.

(83) Baldi, M.; Escribano, V.; Amores, J.; Milella, F.; Busca, G. Characterization of manganese and iron oxides as combustion catalysts for propane and propene. *Appl. Catal. B* **1998**, *17*, L175-L182.

(84) Diehl, F.; Barbier-Jr, J.; Duprez, D.; Guibard, I.; Mabilon, G. Catalytic oxidation of heavy hydrocarbons over Pt/Al_2O_3. Influence of the structure of the molecule on its reactivity. *Appl. Catal. B* **2010**, *95*, 217-227.

(85) Lund, C. R. F.; Kubsh, J. E.; Dumesic, J. A. Water Gas Shift over Magnetite-Based Catalysts: Nature of Active Sites For Adsorption and Catalysis. In *Solid State Chemistry in Catalysis*; Grasselli, R.K., Ed; Brazdil, J.F., Ed.; American Chemical Society: Washington DC, 1985; 279; pp 313-338.

(86) Biesinger, M. C.; Payne, B. P.; Grosvenor, A. P.; Lau, L. W. M.; Gerson, A. R.; Smart, R. S. C. Resolving surface chemical states in XPS analysis of first row transition metals, oxides and hydroxides: Cr, Mn, Fe, Co and Ni. *Appl. Surf. Sci.* **2011**, *257*, 2717-2730.

(87) Ko, T.; Chu, H. Spectroscopic study on sorption of hydrogen sulfide by means of red soil. *Spectrochim. Acta, Part A* **2005**, *61*, 2253-2259.

(88) Descostes, M.; Mercier, F.; Thromat, N.; Beaucaire, C.; Gautier-Soyer, M. Use of XPS in the determination of chemical environment and oxidation state of iron and sulfur samples: constitution of a data basis in binding energies for Fe and S reference compounds and applications to the evidence of surface species of an oxidized pyrite in a carbonate medium. *Appl. Surf. Sci.* **2000**, *165*, 288-302.

(89) Neal, A.; Techkarnjanaruk, S.; Dohnalkova, A.; McCready, D.; Peyton, B.; Geesey, G. Iron sulfides and sulfur species produced at hematite surfaces in the presence of sulfate-reducing bacteria. *Geochim. Cosmochim. Acta* **2001**, *65*, 223-235.

(90) Watanabe, M.; Kato, S.; Ishizeki, S.; Inomata, H.; Smith Jr., R. L. Heavy oil upgrading in the presence of high density water: Basic study. *J. Supercrit. Fluids* **2010**, *53*, 48-52.

(91) Wang, S.; Chung, K.; Masliyah, J. H.; Gray, M. R. Toluene-insoluble fraction from thermal cracking of Athabasca gas oil: Formation of a liquid-in-oil emulsion that wets hydrophobic dispersed solids. *Fuel* **1998**, *77*.

(92) Layng, E. T.; Treating Tar Sands. U.S. Patent 3,151,054, September 29, 1964.

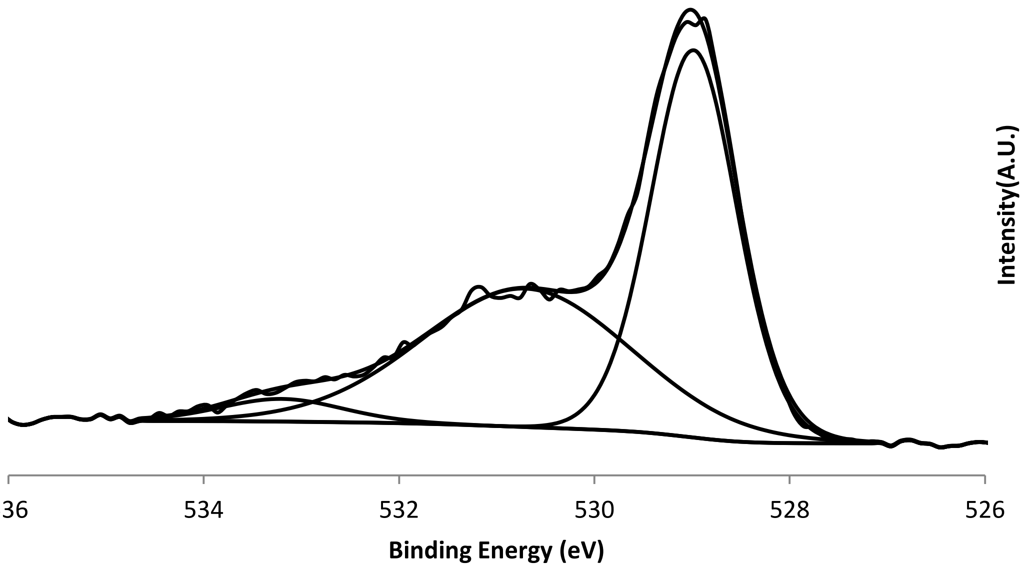

O 1s XPS spectra of feed α-Fe_2O_3 including raw data, overall fitted curve and the individual curves for the three types of oxygen. Oxygen contained in free water at 533.3 eV, hydroxyl surface groups at 530.9 eV and structural O^{2-} at 529.1 eV.

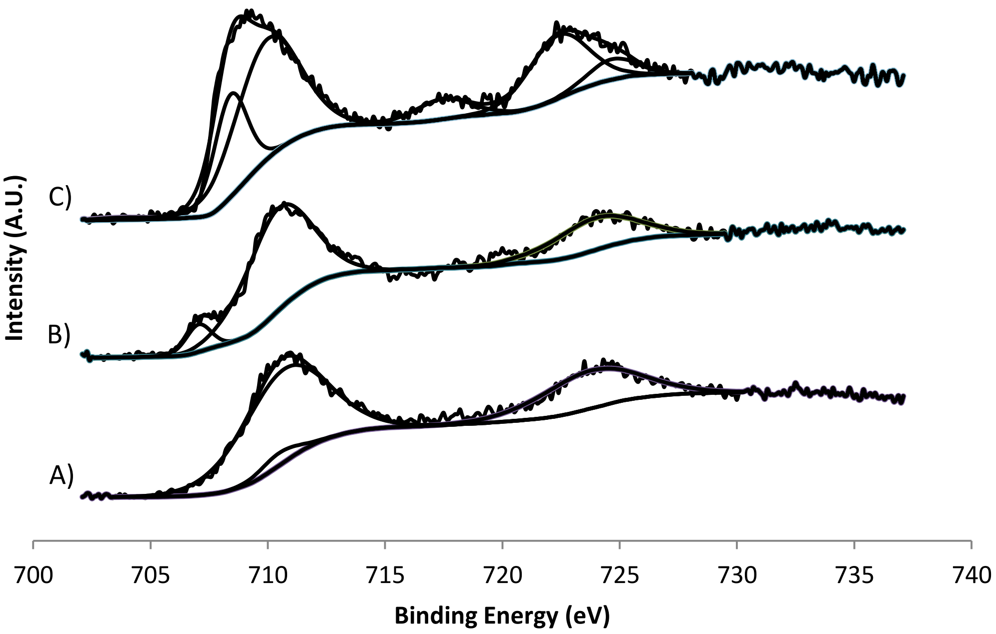

Fe 2p spectrum of the iron oxide catalyst following the cracking of hexadecane and dimethyl disulfide in the a) presence of steam and in the b) absence of steam c) fresh α-Fe_2O_3. Data shown includes raw data, individual fitted curves and overall fitted curve. Peaks at 711 eV is characterized as Fe(III)-O, while peak at 706 eV is characterized as Fe-S.

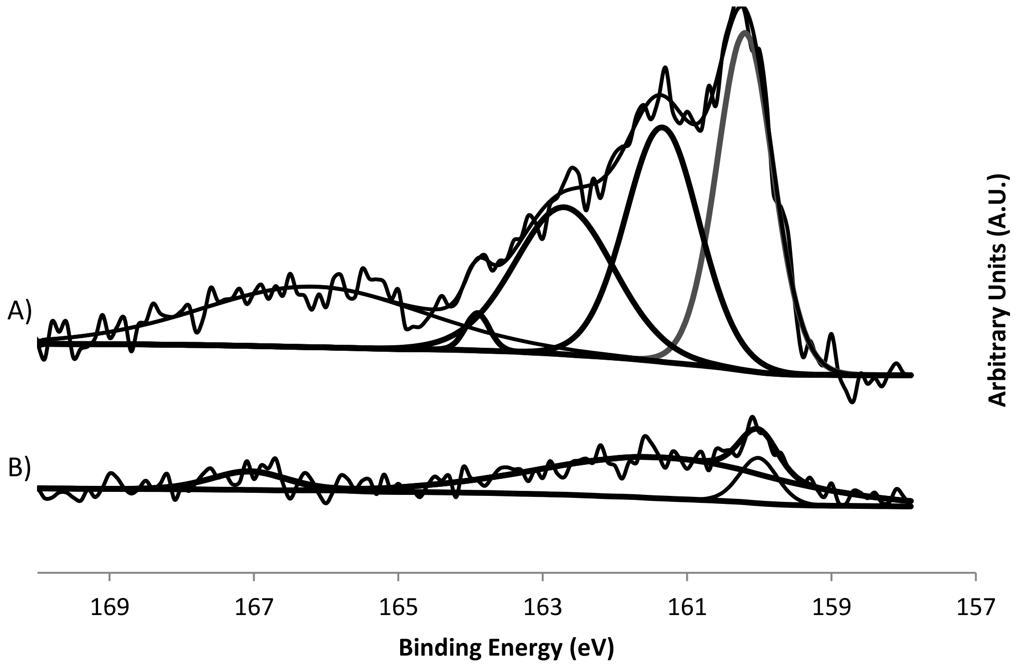

S 2p spectrum of the iron oxide catalyst following the cracking of hexadecane and dimethyl disulfide in the a) absence of steam and in the b) presence of steam. Data represented includes raw data, individually fitted curves and overall fitted curve. The peaks can be identified as FeS (160 eV), Polysulfides (161.5 and 162.9 eV), elemental sulfur (164.1 eV) and sulfates (166 eV).